Journal of Asian Earth Sciences 259 (2024) 105900

Contents lists available at ScienceDirect

Journal of Asian Earth Sciences

journal homepage: www.elsevier.com/locate/jseaes

Changes of tectonic regime of the East China Sea Shelf Basin since Mesozoic: Insights from the Tiantai slope belt, East China Sea

Xinxin Liang [a,b], Shi Chen [a,b,*], Bingshan Ma [c], Baotong Ding [d], Yuanyuan Liang [e], Xingguo Song [a,b], Jianxun Zhou [a,b], Yixin Yu [a,b], Lang Yu [a,b]

[a] National Key Laboratory of Petroleum Resources and Engineering, China University of Petroleum, Beijing 102249, China
[b] College of Geosciences, China University of Petroleum, Beijing 102249, China
[c] School of Geosciences and Technology, Southwest Petroleum University, Chengdu 610500, China
[d] Shenzhen Branch of CNOOC, Shenzhen 518000, China
[e] CNOOC Research Institute, Beijing 100027, China

ARTICLE INFO

Keywords:
East China Sea shelf basin
Tectonic domain transformation
Paleo-Tethys
The Pacific
Tiantai slope belt
Structural modeling

ABSTRACT

Because of its unique tectonic location, the East China Sea shelf basin is an ideal laboratory for studying the transition of the East Asian continent from the Paleo-Tethys tectonic domain to the Pacific tectonic domain. The Tiantai slope belt within the East China Sea shelf basin contains geological information regarding the Mesozoic tectonic system transformation of the basin. Therefore, understanding the structural characteristics and evolution process of the Tiantai slope belt is extremely important. The structural characteristics of the Tiantai slope belt are clarified through the interpretation of seismic data, and its structural model is established. The transition of the East China Sea shelf basin from the Paleo-Tethys tectonic domain to the Pacific tectonic domain is determined. The NWW-trending faults formed in the Jurassic were detachment fault systems. The stress direction shifted during the Early Cretaceous, forming an NE-trending structural feature. The difference in extensional strength between the north and south sides of the Tiantai slope belt allows the NWW-trending basement faults to slip as accommodation faults, regulating deformation and inducing shallow arcuate faults in their hanging wall. The tectonic evolution of the Tiantai slope belt indicates that the East China Sea shelf basin completed the transition from the Paleo-Tethys Ocean tectonic domain to the Pacific tectonic domain in the Early Cretaceous, and the East China Sea shelf basin has entered the back-arc rifting stage of the Pacific tectonic domain after the Jurassic continental marginal depression.

1. Introduction

The East China Sea shelf basin (ECSSB) is located in the primary area where the eastern continental margin of China meets the Pacific plate and is also influenced by the remote effect of the subduction of the Indian plate to the Eurasian plate (Zhang et al., 2016). It is currently a suitable location for studying numerous cutting-edge scientific concerns. Among them, the Cenozoic structure of the basin has been deeply studied, and many valuable research results have been achieved (Dai et al., 2014; Wang et al., 2020; Xu, 2012). Correspondingly, oil and gas exploration has finished a sizable study and achieved a breakthrough (Liang and Wang, 2019; Suo et al., 2014; Wang et al., 2021; Zhang et al., 2016; Zhang et al., 2016; Cukur et al., 2012; Cukur et al., 2011; Tang et al., 2019). However, because the data acquired in the early stages primarily focused on the Cenozoic, the Mesozoic structural framework of the basin is poorly understood (Feng et al., 2003; Liang, 2012; Yang et al., 2019; Yang et al., 2019).

A considerable number of studies have revealed that the South China block experienced a tectonic system shift from the Tethys tectonic domain to the western Pacific tectonic domain during the Mesozoic, although no agreement has been reached on the time of the tectonic system transition (Faccenna et al., 1999; Hou et al., 2015; Li, 2000; Li et al., 2012b,a; Liu et al., 2020; Xu et al., 2019). The ECSSB is located at the southeastern border of the South China plate and its tectonic development dynamics are intimately tied to the kinetic behavior of the ancient Tethys and Pacific plates (Hou et al., 2015). Consequently, it is an important place to investigate the tectonic deformation and dynamic alteration of the South China block. The Tiantai slope belt in the middle

* Corresponding author at: National Key Laboratory of Petroleum Resources and Engineering, China University of Petroleum, Beijing 102249, China.
E-mail address: chenshi4714@163.com (S. Chen).

https://doi.org/10.1016/j.jseaes.2023.105900
Received 4 July 2023; Received in revised form 19 October 2023; Accepted 23 October 2023
Available online 25 October 2023

of the basin is located on a strong NWW basement fault zone, which records the geological information of tectonic system transformation in the ECSSB.

In this study, the tectonic model of the Tiantai slope belt is established using the methodologies of fault activity analysis and equilibrium profile recovery based on careful interpretation of seismic data. The transition time of the ECSSB from the Tethys tectonic domain to the West Pacific tectonic domain is determined by a regional tectonic background study, which is further combined with the research findings of others in recent years.

2. Geological setting

The ECSSB is located on the southeast edge of the Eurasian continent, in the South China block, sandwiched between the Eurasian plate, the Pacific plate, and the Indian plate (Cui et al., 2019). It is adjacent to the Diaoyu Island uplift fold belt in the east and linked to the Minzhe uplift area in the west. It is a Mesozoic–Cenozoic overlaid basin formed on the pre-Mesozoic craton. This basin is distributed in an NNE direction, with a north–south length of about 1100 km, an east–west width of about 325–500 km, and an area of about 26×10^4 km^2 (Chen, 2003).

Numerous studies suggest that the Mesozoic system of the South China block transformed from the EW-trending Tethys tectonic domain to the NE-trending western Pacific tectonic domain (Hou et al., 2015; Li et al., 2012a; Yang et al., 2019a; Yu et al., 2005; Zhang et al., 2009, 2016a; Isozaki et al., 2010). The ECSSB is a part of the West Pacific tectonic domain formed by the successive Indo–Pacific dynamical systems, a part of the Paleo-Asian Ocean tectonic domain formed by the Paleo-Asian Ocean dynamical system, and a part of the Tethys Ocean tectonic domain formed by the Tethys Ocean dynamical system. The formation and evolution of the ECSSB since the Mesozoic and Cenozoic are closely related to the closure of the Paleo-Asian Ocean and the Tethys Ocean as well as the continuous expansion of the Indian Ocean ridge and the subduction of the Pacific plate. The ECSSB contains several NWW-trending faults that are extensions of the continental Qinling orogenic belt to the sea (Fig. 1) (Jiao and Yin, 1987; Suo et al., 2014). These NWW-trending faults in the basin are the products of the Indosinian movement. Currently, the tectonic system of the ECSSB is mainly NE, indicating that the ECSSB has undergone structural domain system transformation.

The basin exhibits east–west zoning and south–north blocking, as well as the structural characteristics of two depressions with one uplift. The West Depression Group, Central Uplift Group, and East Depression Group are the groups from west to east (Li et al., 2012a; Zhang et al., 2014a, 2016a). The West Depression Group comprises the Taibei Depression (containing Qiantang Sag, Jiaojiang Sag, Lishui Sag, and Fuzhou Sag) and the Changjiang Depression (including Kunshan Sag, Changshu Heave, North Jinshan Sag, and South Jinshan Sag). Moving from north to south, the Central Uplift Group comprises the Hupijiao Uplift, Haijiao Uplift, and Yushandong Uplift; from north to south, the East Depression Group comprises the Fujiang Sag, Xihu Sag, and Diaobai Sag (Fig. 2a).

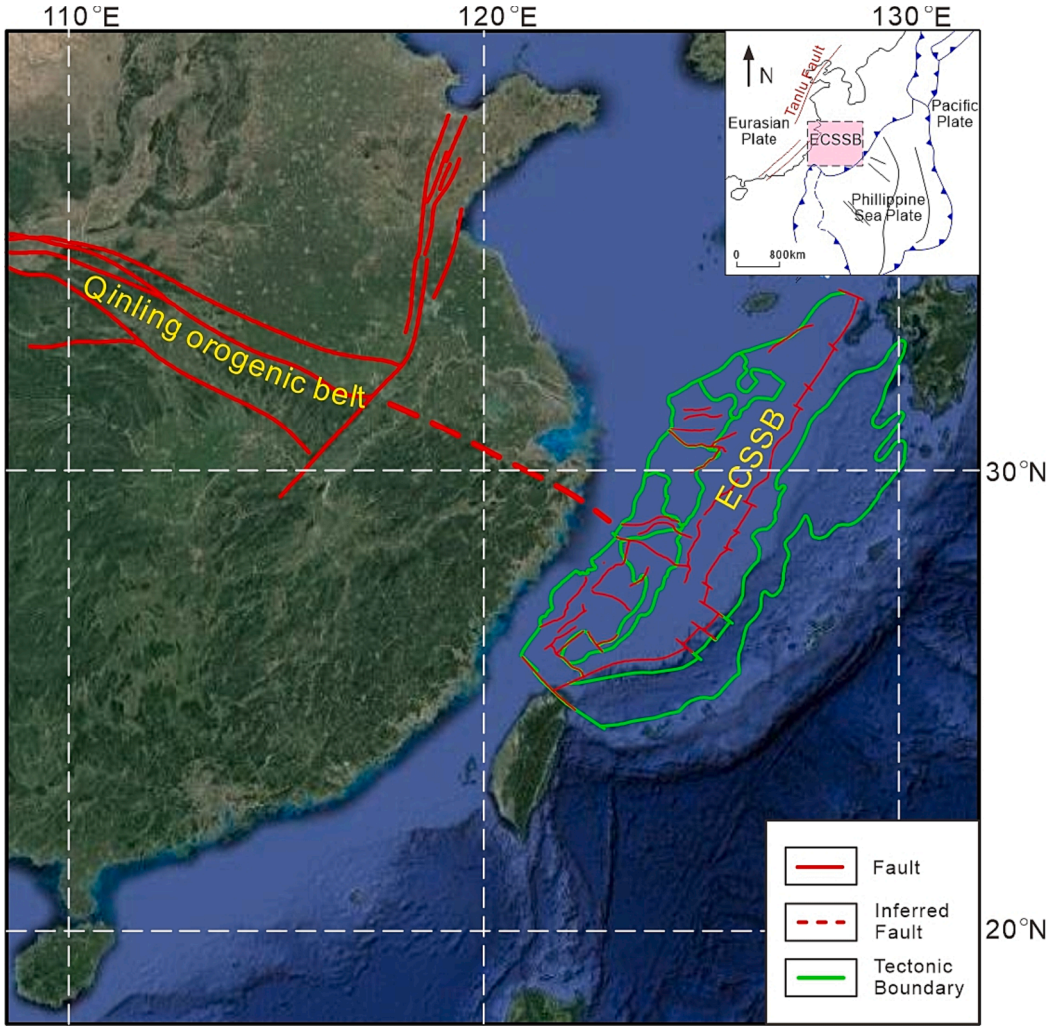

Fig. 1. Satellite map of the East China Sea shelf basin. The Inset map shows the configuration of plates and subduction zones.

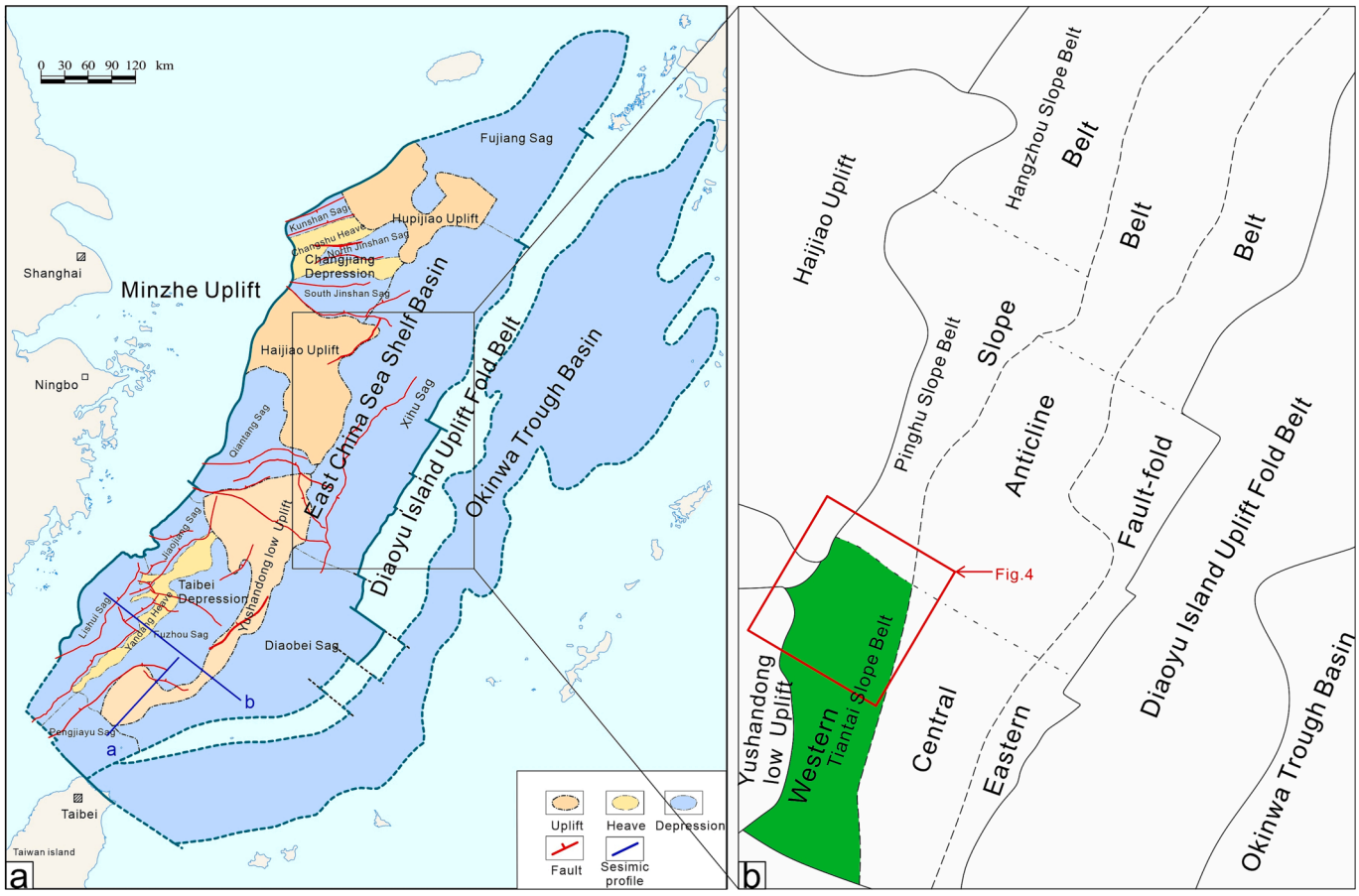

Fig. 2. (a) Map of the East China Sea Shelf Basin; (b) Tectonic map of the Xihu Depression showing the location of the Tiantai slope belt. The study area is outlined by the box in Fig. 2b.

The Xihu Sag is in the East Depression Group of the ECSSB, positioned between the Fujiang Sag and the Diaobai Sag, and it is related to the Diaoyu Island uplift fold belt to the east. The Xihu Sag can be divided into three belts: the western slope belt, middle anticline belt, and eastern fault-fold belt. From north to south, the western slope belt is separated into three sections: Hangzhou slope belt, Pinghu slope belt, and Tiantai slope belt (Zhang et al., 2014). The Tiantai slope belt, covering an area of approximately 3100 km^2, is located to the south of the western slope belt. It lies between the Yushan uplift and the major depression of the Xihu Sag and is bordered to the north by the Pinghu slope belt, to the south by the Diaobai Sag, and to the east by the central anticline belt (Fig. 2b).

Drilling and seismic data provide insights into the Cenozoic strata in the Tiantai slope belt. The stratigraphic sequence from bottom to top includes the Upper Cretaceous, Paleocene (T100–T90), Eocene Bajiaoting Formation (T80–T50), Baoshi Formation (T50–T40), Pinghu Formation (T40–T30), Oligocene Huagang Formation (T30–T20), Miocene Longjing Formation (T20–T16), Yuquan Formation (T16–T12), Liulang Formation (T12–T10), Pliocene Santan Formation (T10–T0), and Quaternary Donghai Formation (T0–present). These strata correlate with the four key tectonic evolution stages of the Xihu Depression, namely the late Cretaceous–early Eocene rifting stage, the middle–late Eocene rifting–depression stage, the Oligocene–Miocene compression inversion stage, and the Pliocene regional subsidence stage (Fig. 3).

3. Structural characteristics of the Tiantai slope belt

The fault trends in the research region are mainly divided into NE, NWW, and arcuate faults with strike transformation. The NE direction represents the main distribution of faults in the area (Fig. 4). Based on the characteristics of fault plane distribution, the study area exhibits distinct features. The faults in the northern and southern extension areas are NE-trending normal faults, with the northern Tiantai slope belt as the transitional site between them. The influence of the basement fault zone has resulted in the development of a series of NE–NW–NWW arcuate faults along the NWW-trending basement fault zone. A detailed analysis of the faults in the Tiantai slope belt is conducted using 2D and 3D seismic data in conjunction with gravity and magnetic data.

Based on the scale, the faults in the research region can be classified into three tiers. The main faults are boundary faults that control the sag and are characterized by large throw, long extension, early formation time, and prolonged activity time. The main faults in the study area include the Pinghu fault (Fig. 4 (EF1)), the Tiantaixi fault (Fig. 4 (WF1)), and the Baoshi fault (Fig. 4 (EF2)). Secondary faults play a regulatory role in forming the structural belt within the sag, exhibiting substantial throw, extended extension, and prolonged duration. The secondary faults in the study area comprise EF3, EF4 and EF5, and other faults. Tertiary faults refer to faults that control local structures and have minimal impact on sedimentary environments. They are characterized by small throws and a small scale. The studied region contains numerous developed tertiary faults (Fig. 4).

3.1. Fault characteristics

3.1.1. Identification and characteristics of basement NWW-trending faults

There are many NWW-trending dominant and recessive faults in the Tiantai slope belt, and the NE-trending fault is consistent with the main direction of the sag arcs along the NWW-trending fault. The shallow igneous rocks also exhibit a northwest-trending bead-like spreading (Fig. 4).

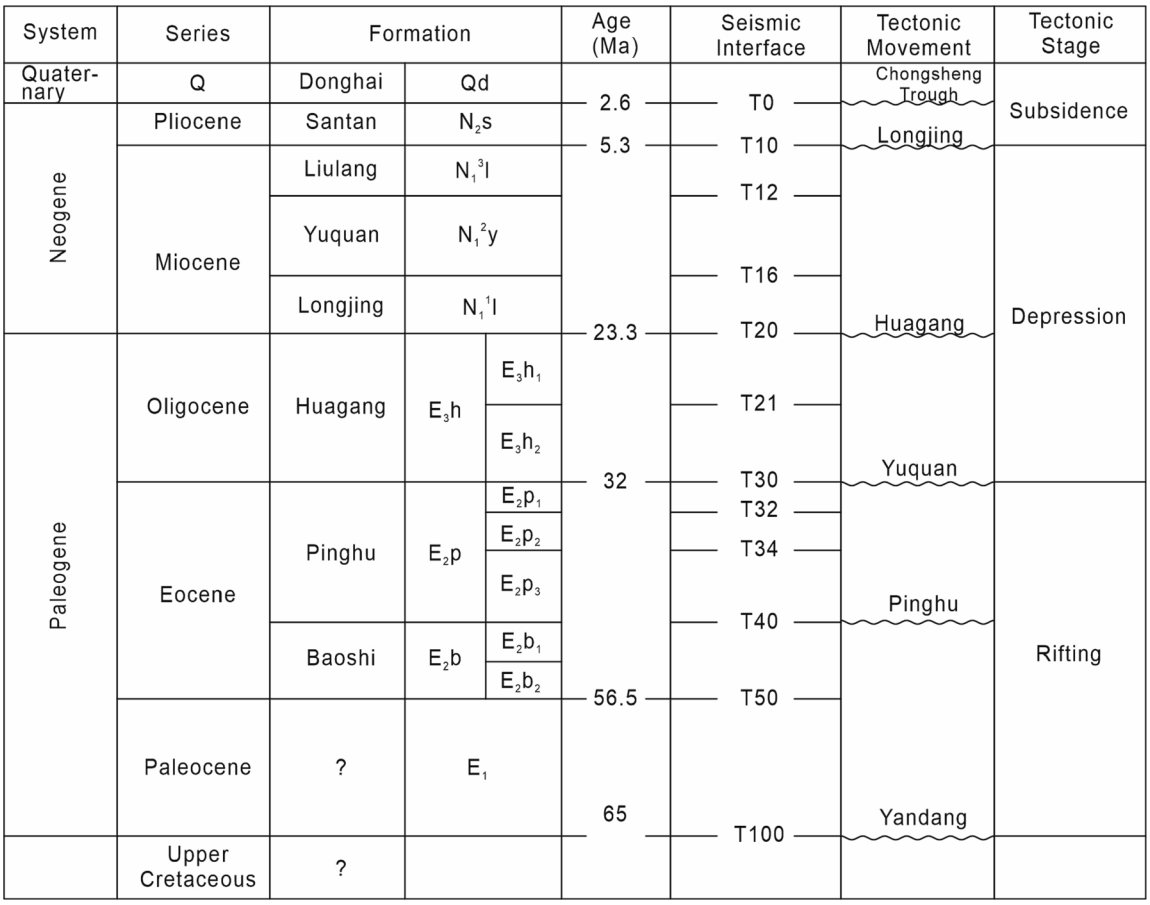

Fig. 3. Comprehensive stratigraphic column of the Xihu Sag showing the stratigraphy, the seismic reflecting surfaces (horizons), and the timing of regional tectonic stages.

(1) NWW-trending fault identification

Identifying NWW-trending basement faults in Xihu Sag is challenging due to their early formation age, thick overburden, and other factors. This group of faults is nearly perpendicular to the tectonic strike, making them relatively subtle and difficult to detect in seismic data. However, they are reflected in gravity and magnetic data.

Gravity and magnetic anomalies can be used to delineate these faults. Abnormal staggering or twisting of faults can be observed in gravity and magnetic fields, and beaded magnetic anomalies are distributed along both sides of the faults. However, not all faults will be reflected in the gravity and magnetic anomalies, particularly those with small scale, low density, and minimal magnetic differences on both sides. The strata on the two walls of the fault exhibit horizontal differences in magnetism and density, which should be evident in gravity and magnetic anomalies. This provides the geophysical basis for determining the strike and plane positions of the fault using gravity and magnetic anomalies.

Multiple low-magnetic anomaly zones are present in the basement of the East China Sea basin. Based on gravity, magnetic, and seismic data, 25 faults have been identified (Fig. 5). Based on the faults' directions, they are divided into two groups: NE and NWW. The NWW-striking fault is particularly prominent in the Tiantai slope belt, and the low magnetic anomaly zone may be the deep sedimentary rock series, representing the distribution direction of the Mesozoic basin.

(2) NWW-trending fault characteristics

The Tiantaixi fault (Fig. 4 (WF1)) is an obvious NWW basement fault that starts from the Yushan low uplift in the west, deflects eastward to the NNW, runs through the Tiantai slope belt, and extends for more than 40 km. The fault is normal, with a steep top section and a mild bottom section, along with an NNE dip. It cuts down into the basement and breaks up at the T10 interface. The seismic data show that the Tiantaixi fault has obvious control over the Mesozoic period. The footwall stratum of the fault is substantially thinner than the hanging wall stratum. It is characterized by a half graben–like dustpan and rolling anticlines are developed. The deep form of the Tiantaixi fault is restored using the vertical simple shear theory in conjunction with the development characteristics of the rolling anticline in the hanging wall of the fault. Further, the Tiantaixi fault is considered to be a detachment fault (Fig. 7).

On the hanging wall of the Tiantaixi fault, multiple tiny normal faults (Figs. 6 and 7 (WF3-7)) with NWW-trending parallel to the Tiantaixi fault are also found. Unlike the Tiantaixi fault, which is active to the Cenozoic period, these faults only developed in the Mesozoic period, with steep upper and gentle lower sections, converging downward on the detachment plane of the Tiantaixi fault. The Mesozoic strata controlled by these faults are faulted in the southern part and overlapped in the northern part. The sedimentary characteristics are the same as those controlled by the Tiantaixi fault.

Gushan fault is an NWW-trending recessive fault (Figs. 4 and 6 (WF2)). The western section of the fault is similar to the Tiantaixi fault and is a Mesozoic active normal fault with a steep top section and a mild bottom section, a large number of Cenozoic arcuate faults develop in the hanging wall (Fig. 8a). In plane view, near Gushan fault, the strike of shallow fault changes, gradually changing from NE to NWW (Fig. 4 (EF3-5)). The eastern section of the Gushan fault is an upright strike-slip

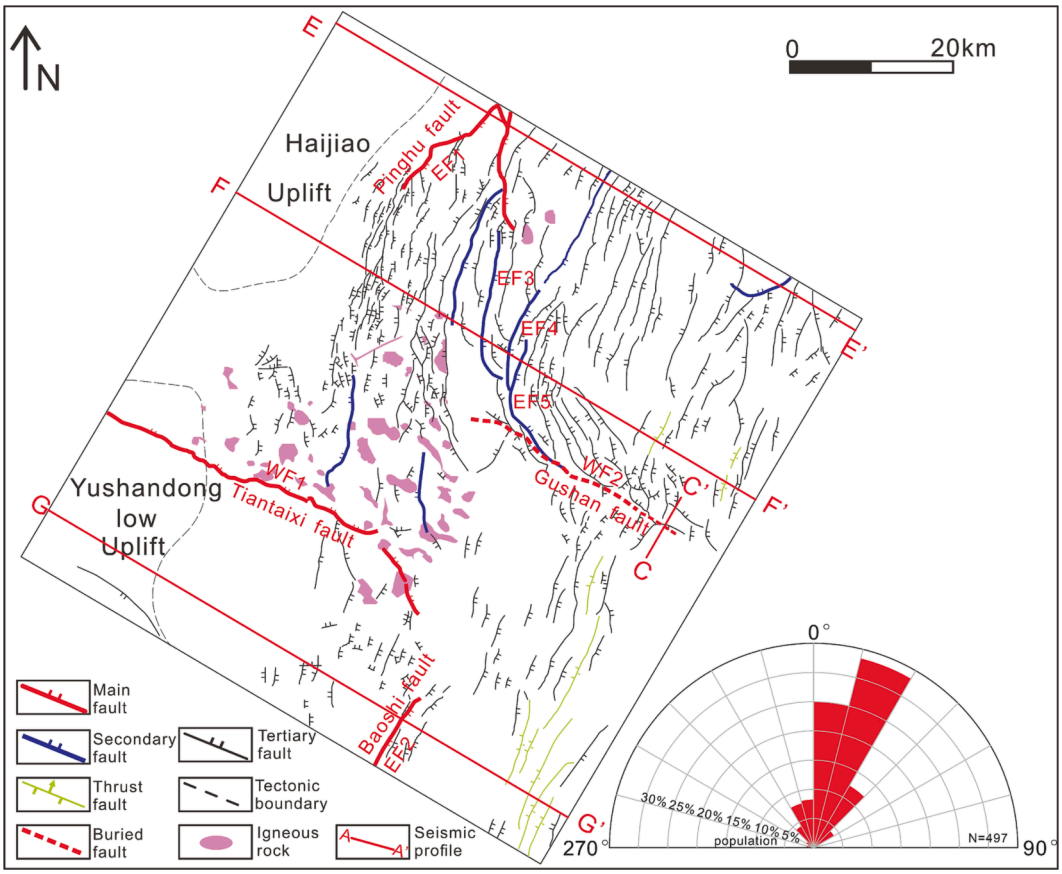

Fig. 4. Plane geometric characteristics of fault systems based on 3D seismic interpretation of the T30 horizon and fault strike azimuth frequency distribution in the Tiantai slope belt. See the location in Fig. 2b. WF1: Tiantaixi fault, WF2: Gushan fault, EF1: Pinghu fault, EF2: Baoshi fault, EF3-5: Shallow arc fault.

fault, with flower-like structure visible in the section and braided structure visible in the plane (Figs. 4 and 8b). The difference between the eastern and western segments of the Gushan fault indicates that the eastern segment of the fault should be the product of the Mesozoic era, and it may be the same fault system as the western Tiantai fault. During the continuous activity of the Cenozoic, it gradually extended westward and formed a typical strike-slip fault.

The structural attributes of the NWW-trending fault system of the Tiantai slope belt are determined by analyzing the NWW-trending basement fault. It is considered that the NWW-trending basement fault in the Tiantai slope belt is a deep detachment fault system dominated by the Tiantaixi fault. Several detachment faults with the same dip form a dustpan-like half-graben structure in the hanging wall of the Tiantaixi fault, influencing Mesozoic sedimentation. Several normal faults form a horst–graben structure with the opposite dip to the south of the Tiantai slope belt (Figs. 9 and 10).

3.1.2. NE-trending fault characteristics

The Tiantai slope belt has a high density of NE-trending faults, with the main faults being the Pinghu fault and the Baoshi fault, which control the slope.

The Pinghu fault (EF1) is located west of the southern Pinghu slope belt, controlling the development of the southern Pinghu slope belt, and the south side of the fault runs all the way to the Tiantai slope belt. It has an arc-shaped plane. On the profile, the fault dips to the southeast, cutting through the Mesozoic basement downward and the shallow layer upward. It exhibits a steep upward and gentle downward inclination, resembling a shovel-type normal fault with a high angle. This fault considerably influences sedimentation and creates a sliding fault step with a series of secondary faults in the hanging wall (Fig. 11a).

The Baoshi fault (EF2), located on the east side of the Tiantai slope belt, controls the development of the Tiantai slope belt and is distributed in the NE trending on the plane. The fault profile displays a high-angle shovel-type normal fault that deeply penetrates the basement downward and cuts through the shallow layer upward. It also has an obvious sedimentation-control effect (Fig. 11c).

In addition to the aforementioned main faults, the Tiantai slope belt also contains numerous small-scale and discontinuous NE-trending faults (Figs. 4 and 11b). These fault profiles are characterized by shovel-type normal faults with a steep upper portion and a gentle lower portion. They dip to the east and west, cutting down to the basement and mostly terminating at the T21 interface (Fig. 11a and 11b). The strike gradually changes from NE to nearly SN to NW on the plane, forming an arcuate fault.

3.1.3. Relationship between deep and shallow fault systems

The Tiantai slope belt has undergone multiple stages of rifting, along with the Xihu Sag, resulting in distinct differences between the fault systems of different strata.

Mesozoic bottom interface (Tg surface): the dominant fault system is a detachment fault system dominated by the Tiantaixi fault. It exhibits a series of NWW-trending nearly parallel fault combinations on the Mesozoic bottom, dipping NEE. The Tiantaixi fault has the longest extension (Fig. 6).

Bottom interface of the Pinghu Formation (T40 surface): the faults in the Pinghu Formation are primarily NE-trending faults; NWW-trending faults are basically not developed and only the Tiantaixi fault remains active at this interface. Toward the north of the basement NWW-trending fault, the trend of shallow NE-trending faults changes from NE–SN–NWW, and on the plane, they appear as an arc fault (Fig. 12a).

Bottom interface of the lower section of the Huagang Formation (T30 surface): the fault system at the bottom interface of the lower section of

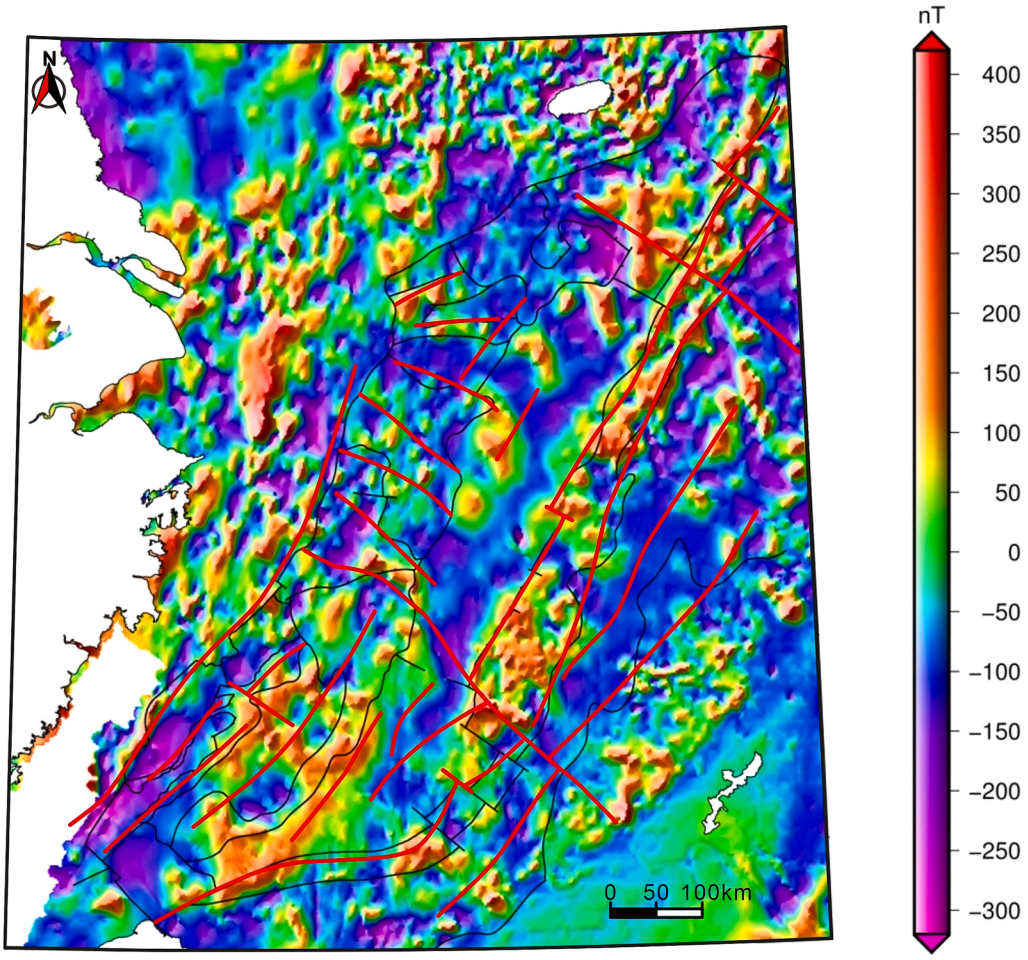

Fig. 5. Geomagnetic anomaly map of the East China Sea basin (derived from Shanghai Branch of CNOOC Ltd).

the Huagang Formation is similar to the bottom interface fault system of the lower section of the Pinghu Formation, which is a Cenozoic-developed fault continuously active at this layer. NE-trending faults dominate and converge in an arc-like manner near the NWW-trending basement fault site (Fig. 4).

By comparing the fault systems of different strata, it is evident that shallow faults are separated by NWW-trending basement faults, resulting in the overall north–south zoning of Cenozoic faults. Shallow faults far from the NWW-trending basement faults are primarily linear NE-trending normal faults. However, the trend of faults near the basement changes to arc faults. This trend change mainly occurs in the hanging wall of the basement fault, particularly to the north of the Gushan fault. The profile reveals that shallow faults are concentrated in the hanging wall of the Gushan fault and are largely absent in its footwall (Fig. 8a and 12b).

3.2. Fault activity time

The seismic data in the time domain is transformed into the depth domain using the time-depth conversion equation, and the paleo-throw of the fault is derived. This study quantitatively characterizes the activity of the major NE and NWW faults in the Tiantai slope belt by analyzing fault paleo-throw data. The activity time of these fault groups in the study area is determined by combining the relevant findings of previous studies on fault activity.

3.2.1. NWW-trending fault activity

The NWW-trending faults in the Tiantai slope belt are primarily concealed faults, located deep in the basement and detachment zone. Only the Tiantaixi fault has remained active during the Cenozoic period. Due to limited drilling data, it is impossible to determine the specific Mesozoic strata involved. However, Mesozoic tectonic evolution can be inferred based on regional correlation and analysis of the hanging wall strata of NWW-trending basement faults. The activity of the Tiantaixi fault during the Cenozoic era is also established.

The Jurassic and Cretaceous systems, represented sequentially by the Fuzhou Formation of the Middle Lower Jurassic, the Xiamen Formation of the Upper Jurassic, the Lower Cretaceous Yushan Formation, and the Minjiang Formation Shimentan Formation of the Upper Cretaceous from bottom to top, constitute the Mesozoic residual strata in the ECSSB. Previous studies on Mesozoic residual basins (Li et al., 2015; Zhong et al., 2019) support this classification.

Based on the interpretation and comparison of seismic reflection waves from the seismic profile in the south of the ECSSB, the estimated thickness of the Mesozoic is approximately 2500–5000 m. The internal seismic facies also exhibit distinct differences from the seismic facies characteristics of the corresponding Cenozoic strata in the upper part. The sedimentary thickness of the Jurassic and Cretaceous systems is regulated by NWW-trending faults. The structure is characterized by a fault depression that resembles a dustpan, faulted in the south but overtopped in the north (Fig. 13a)(Liang, 2012), which is consistent with the NWW-trending fault pattern of the Tiantai slope belt.

The study of Mesozoic faults in the southern part of the ECSSB and Hangzhou Bay area reflects the formation of the NWW-trending extensional fault system in the ECSSB during the Mesozoic. Mesozoic sedimentation is governed by NWW-trending faults, and the Mesozoic

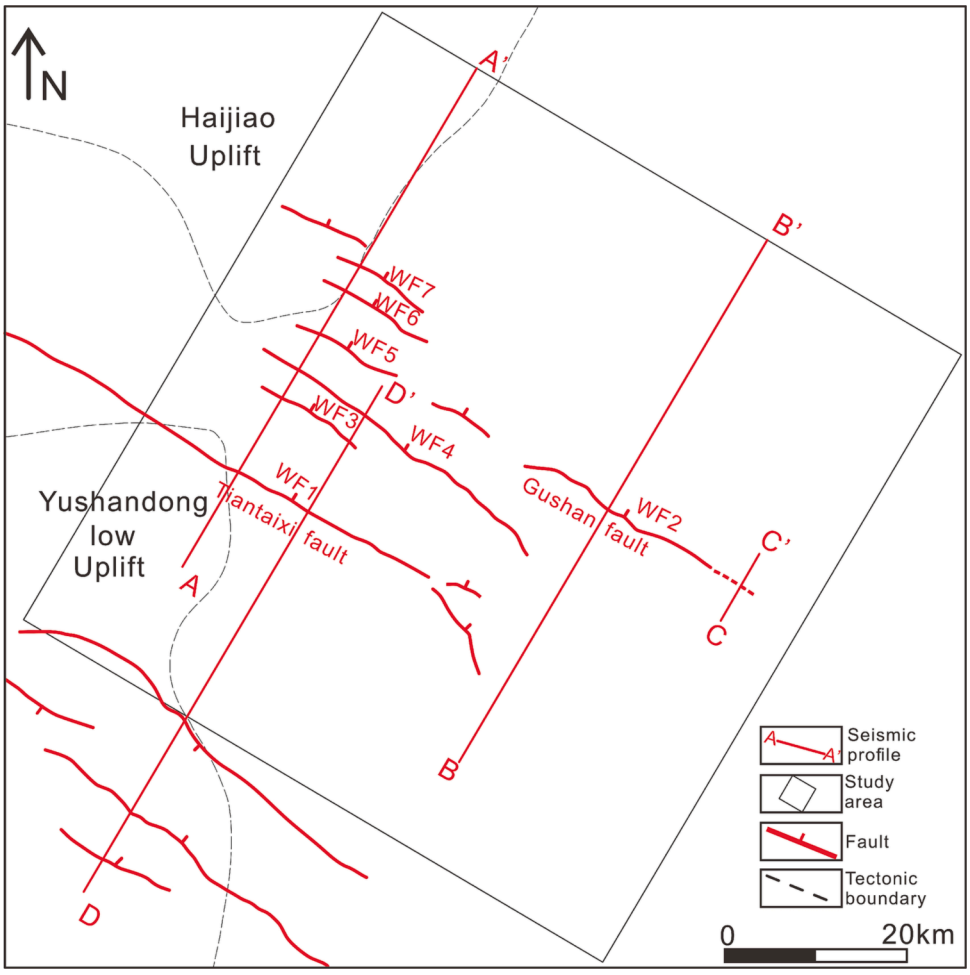

Fig. 6. Basement fault system of the Tiantai slope belt, based on 3D seismic interpretation of Tg horizon. WF1: Tiantaixi fault, WF2: Gushan fault,

sedimentation under their control is primarily recognized by a fault depression resembling a dustpan that is faulted in the south and overlaps in the north. Since the Cretaceous and Jurassic are part of the Mesozoic residual basin strata in the ECSSB, and NWW-trending faults can be seen there to control the distribution of the Jurassic system (Fig. 14a), while the Cretaceous mainly have an NE-trending distribution and was controlled by NE-trending faults (Fig. 14b) (Zhong et al., 2019), it is assumed that they have been present since the Jurassic.

Only the Tiantaixi fault is active from the Mesozoic to the Cenozoic of the Tiantai slope belt NWW-trending faults, and the secondary detachment normal fault of its hanging wall did not cut through T100. Therefore, the activity of NWW-trending faults is analyzed based on the paleo-throw statistics of the Tiantaixi fault. The fault activity data indicate that the Tiantaixi fault was active throughout the Cenozoic, primarily during Paleocene and Early Eocene ($E_1 + E_2b$) and the lower Pinghu Formation sedimentary period (E_2p_3). The activity diminished when the lower Pinghu Formation was deposited, although it remained active until the sedimentary epoch of the Liulang Formation (N_1^3l) (Fig. 15).

3.2.2. NE-trending fault activity

Pinghu fault and Baoshi fault, two sizable NE-trending depression control boundary faults, have formed in the north and south of the Tiantai slope belt, respectively. Owing to the lack of drill data, it is difficult to determine the Mesozoic in Xihu Sag and the existing data can only support the development process of faults from the Cenozoic. The Late Triassic - Jurassic in the ECSSB is a depressional deposit in the Mesozoic based on previous analysis of the NE-trending fault seismic profile across the southern part of the ECSSB, and the Cretaceous system is a half-graben-like filling with a fault in the east and overlap in the west as well as thick in the east and thin in the west (Yang et al., 2020; Yang et al., 2019). In general, the Jurassic structure is wide and gentle and the fault cutting through the Jurassic basically does not control the thickness of the Jurassic system but controls the thickness of the Cretaceous system; that is, the NE-trending fault has mostly developed since the Cretaceous period (Fig. 13b).

The statistical results of the paleo throw of the fault show that the Pinghu and Baoshi faults had multiple periods of activity in the Cenozoic era. The Baoshi fault was active in the upper part of the Huagang Formation (E_3h_1). The Pinghu fault was active for a long time and the Yuquan Formation (N_1^2y) was still active. The main active period in the Cenozoic era is Paleocene and Early Eocene. The activity of the Baoshi fault is much weaker than that of the Pinghu fault. The paleo throw of the Pinghu fault in $E_1 + E_2b$ can reach 6000 m, while the highest of the Baoshi fault is less than 1000 m (Fig. 16).

4. Discussion

4.1. Establishment of the Tiantai slope belt structure model

Statistics on the activity of the main faults on the north and south sides of the Tiantai slope belt demonstrate that the activities of the main sag–controlling faults on the north and south sides of the Tiantai slope belt are clearly different. The paleo throw of the Pinghu fault in the same stratum is greater than that of the Baoshi fault, which reflects that the extension amount on the north side of the Tiantai slope belt is greater

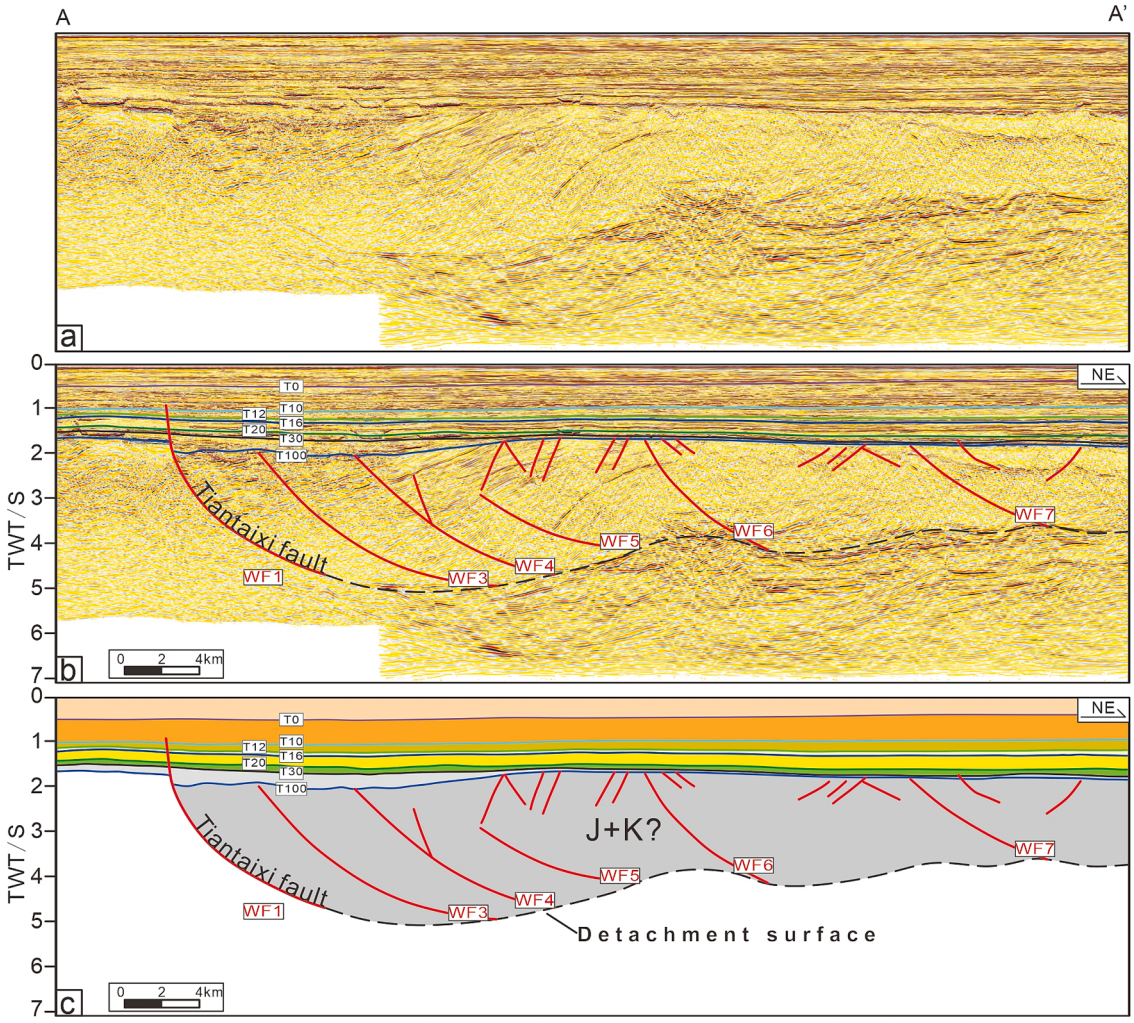

Fig. 7. (a) Uninterpreted and (b) interpreted seismic profiles and (c) structural profile in the direction of NE–SW across the Tiantaixi fault (profile positions shown in Fig. 6). The Tiantaixi fault (WF1) is a detachment fault with rolling anticline and multiple secondary faults (WF3-7) developed on the hanging wall.

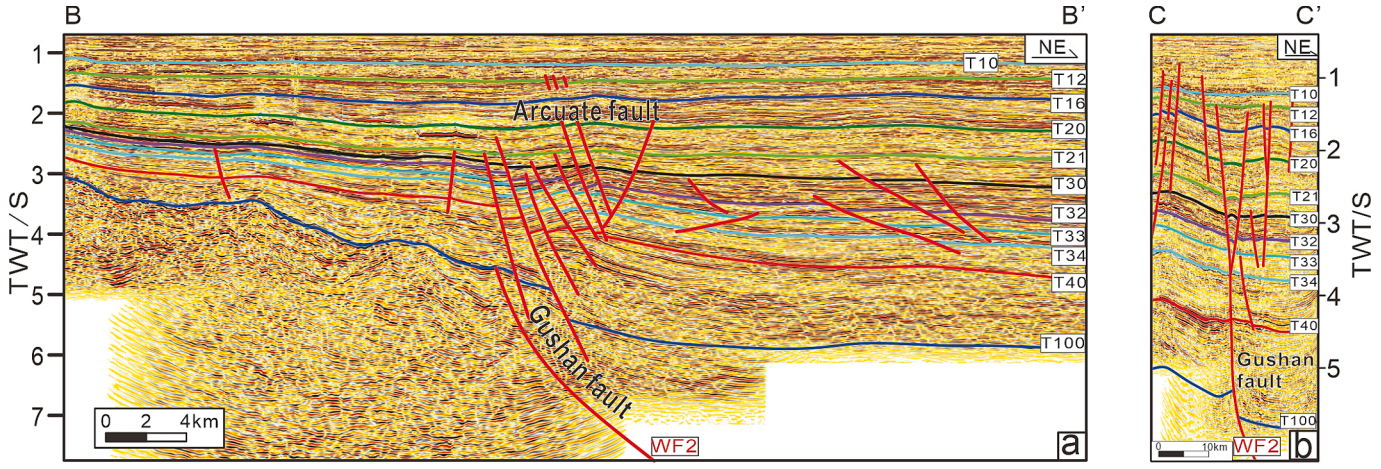

Fig. 8. Typical seismic profiles in the direction of NE–SW across the Gushan fault (profile positions shown in Fig. 6). (a) Normal fault in the western section, the hanging wall of the Gushan fault developed a great number of shallow arcuate faults. (b) The strike-slip fault in the eastern section developed flower-like structure.

than that on the south side. To accurately determine the difference between the two sides, one evolution profile (EE') is selected from the Pinghu fault and one (GG') from the Baoshi fault. Further, the extension amount for different periods is calculated. The maximum extension amount across the Pinghu fault is 4.15 km (8.6%) in Paleocene and Early Eocene ($E_1 + E_2b$) (Fig. 17). The Cenozoic maximum extension of the Baoshi fault is also in Paleocene and Early Eocene ($E_1 + E_2b$), but only 0.25 km (0.7%) (Fig. 17). The comparison results of extension amount

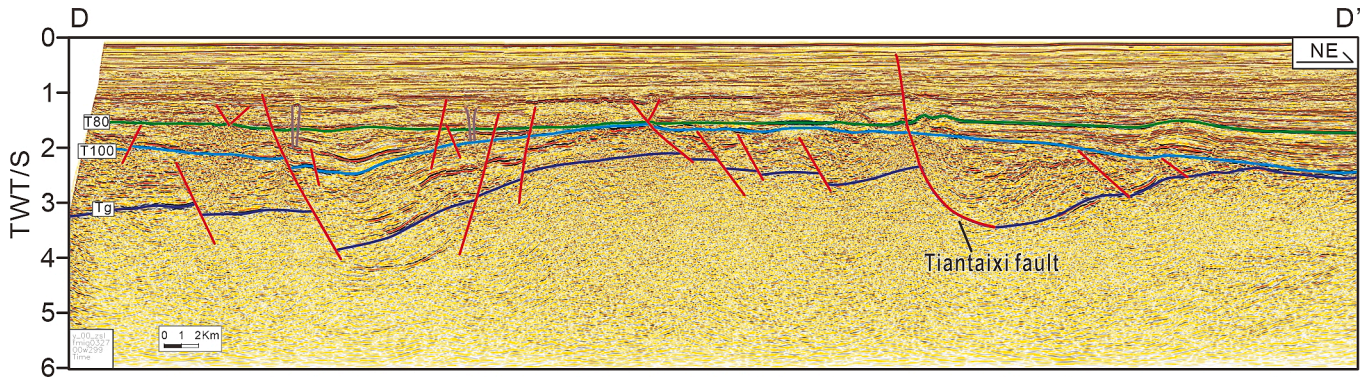

Fig. 9. Typical seismic profile in the direction of NE–SW across the Tiantai slope belt (profile positions shown in Fig. 6). Several normal faults form a horst–graben structure with the opposite dip on the south of the Tiantai slope belt.

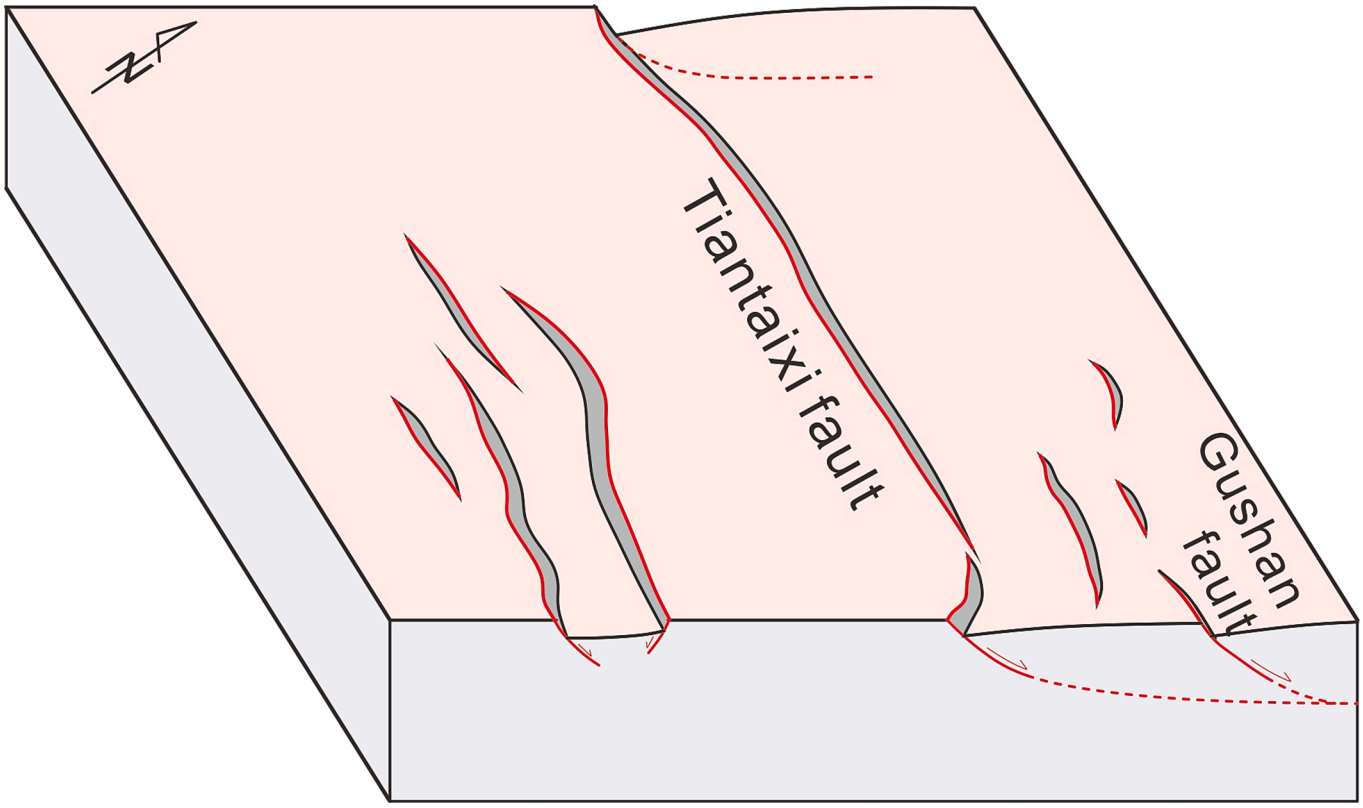

Fig. 10. Mesozoic structural model of the Tiantai slope belt. The NWW-trending basement fault in the Tiantai slope belt is a deep detachment fault system dominated by the Tiantaixi fault.

show that the extension intensity in the north of the slope is greater than that in the south, and the maximum difference of extension amount is about 3.9 km in $E_1 + E_2b$.

The NWW-trending basement fault of the Tiantai slope belt is a detachment fault system. By comparing it with the surrounding Mesozoic residual basin strata, it is assumed that the sedimentary strata in the hanging wall of the basement fault are Jurassic and Cretaceous. The Lower Jurassic Fuzhou Formation, with the lithology generally consisting of gray–black mudstone and silty mudstone (Li et al., 2015; Liu et al., 2020). It is speculated that this plastic layer serves as the detachment surface of the basement extension detachment system in the Tiantaixi fault.

The fault system of the Tiantai slope belt is complex and multiple faults superpose to form a complex structural system. The NWW-trending faults in the early stage are detachment fault systems (Fig. 18a), and the direction of extension stress changes, resulting in the NE-trending structural feature of the Tiantai slope belt. The extension strength in the north of the Tiantai slope belt is greater than that in the south. In an environment where the north–south extension strength differs, the NWW-trending basement faults reactivated as accommodation faults, among them, the strike-slip activity of the Gushan fault is the most obvious, and the typical strike-slip fault features can be seen in its eastern section. Under the action of strike-slip activities, the hanging wall of Mesozoic normal faults in the eastern section is an active sliding plate, and a series of Riedel shears are formed on the hanging wall, which intersects with the primary displacement zone at a small Angle. The Angle between the Riedel shears and the primary displacement zone indicates that the basement fault has dextral strike-slip activities. The continuous strike-slip activity connected these near S-N Riedel shears with NEE faults, forming the Cenozoic arcuate faults (Fig. 18b).

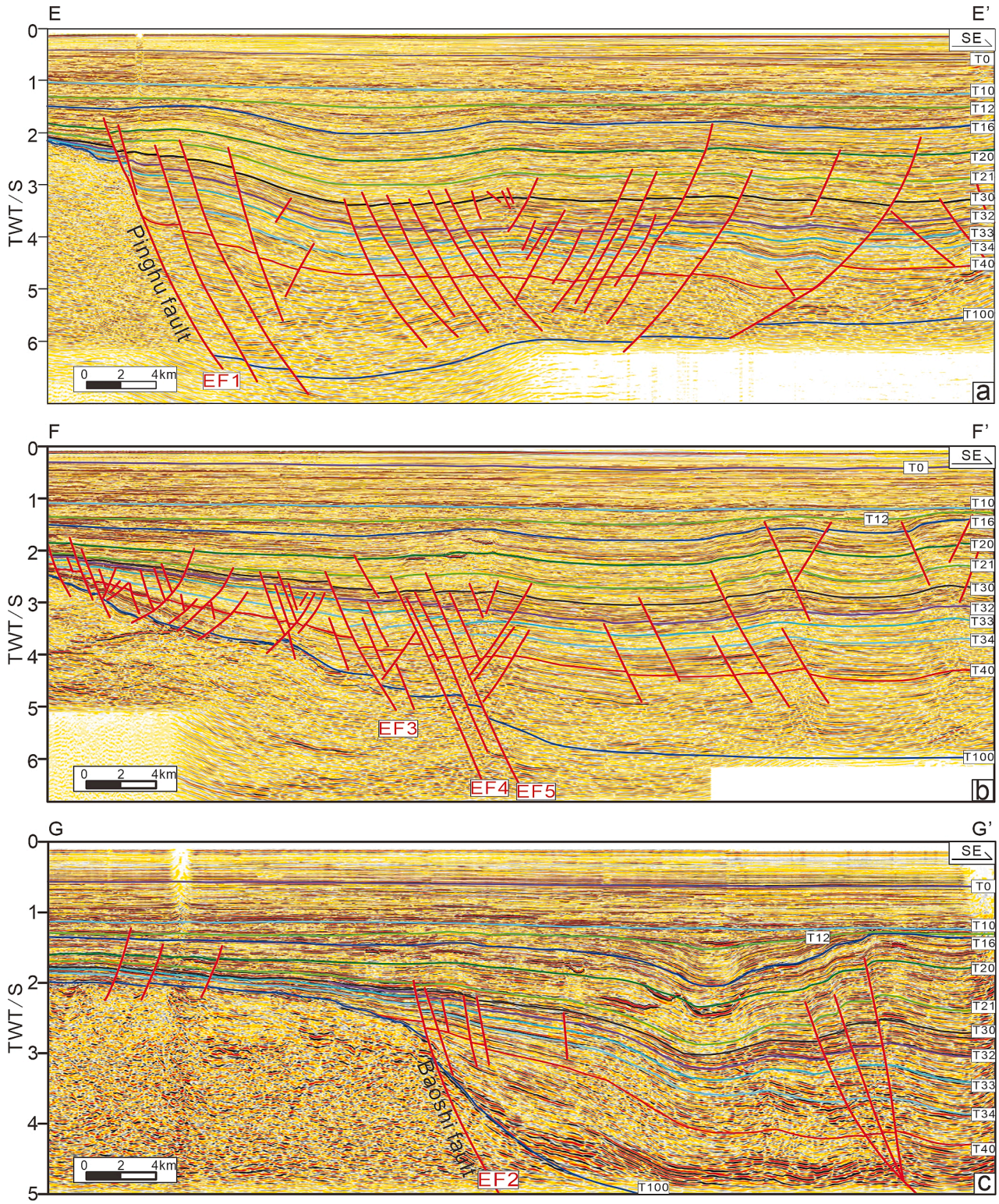

Fig. 11. Typical seismic profiles in the direction of NW-SE across the Tiantai slope belt (profile positions shown in Fig. 4).

4.2. Tectonic evolution of the Tiantai slope belt

By analyzing the activity of various fault systems in the Tiantai slope belt, the fault systems in each structural stage of the Tiantai slope belt can be separated from the current complex superposition effect caused by multiple tectonic activities. The evolution of the Tiantai slope belt can be reconstructed when combined with the structural model of the research region, which can be divided into four stages: the incubation period, initial period, mature period, and quiet period.

Incubation period (Jurassic): the NWW-trending faults mentioned above were mainly active during the Jurassic period. At this time, NW-trending basement detachment normal faults were developed, and the hanging wall deposited the Jurassic system, providing a basis for conversion (Fig. 19a).

Initial stage (Cretaceous–Early Eocene Epoch): the tectonic stress reversed the direction of the basin, generating a sequence of NE-trending

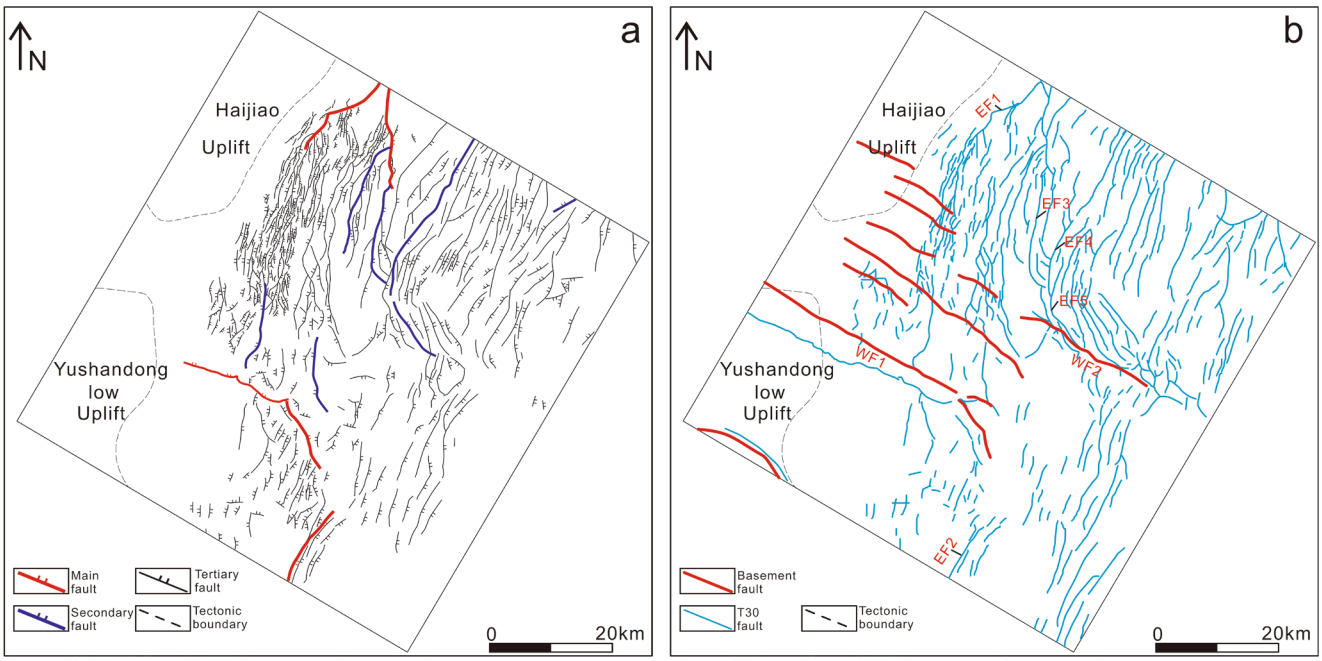

Fig. 12. (a) Plane geometric characteristics of fault systems of the T40 horizon in the Tiantai slope belt. (b) Superimposed Diagram of fault systems based on the T30 and Tg horizons in the Tiantai slope belt. Shallow faults (EF3-5) far from the NWW-trending basement faults are primarily linear NE-trending normal faults. However, the trend of faults near the basement changes to arc faults.

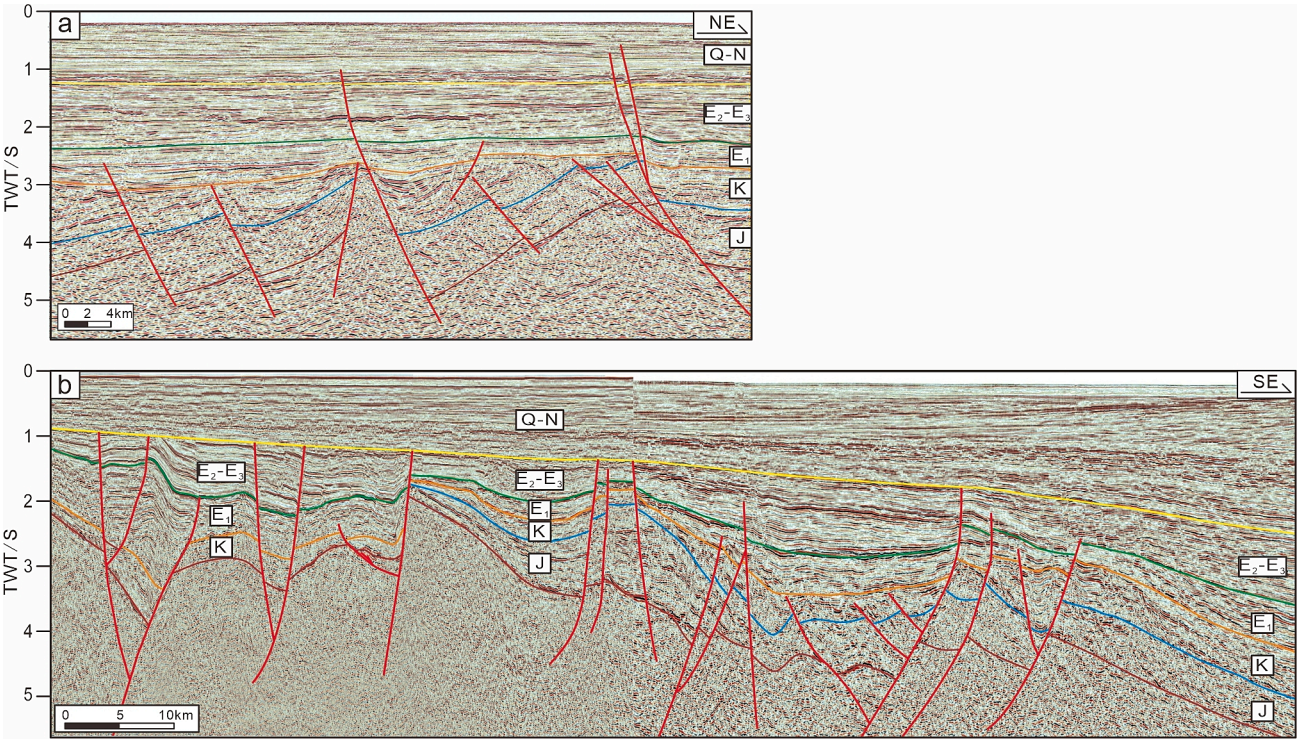

Fig. 13. Typical geological profiles in the southern East China Sea shelf basin (profile positions shown in Fig. 2). (a) The characteristics of NWW-trending fault were shown, the Jurassic and Cretaceous deposits are controlled by the NWW faulting, which is faulted in the south but overtopped in the north (Modified after Liang, 2012). (b) The characteristics of NE-trending fault were shown, the fault cutting through the Jurassic basically does not control the thickness of the Jurassic system but controls the thickness of the Cretaceous system (Modified after Yang et al., 2019).

faults. The strike–slip activity of the basement fault was caused by the differential extension of the north and south sides of the Tiantai slope belt. The strike–slip movement of the basement fault caused the NE-trending fault in the hanging wall to converge toward the basement fault near the plane of the basement fault, forming an arc fault, at this time, the arc fault activity is relatively low (Fig. 16). The sedimentation was mostly unaffected by the NW-trending basement fault (Fig. 19b).

Maturity period (Late Eocene): the activity of the arc fault increased gradually compared with the initial period (Fig. 16), the basement fault exhibited high strike–slip activity, forming numerous arc faults

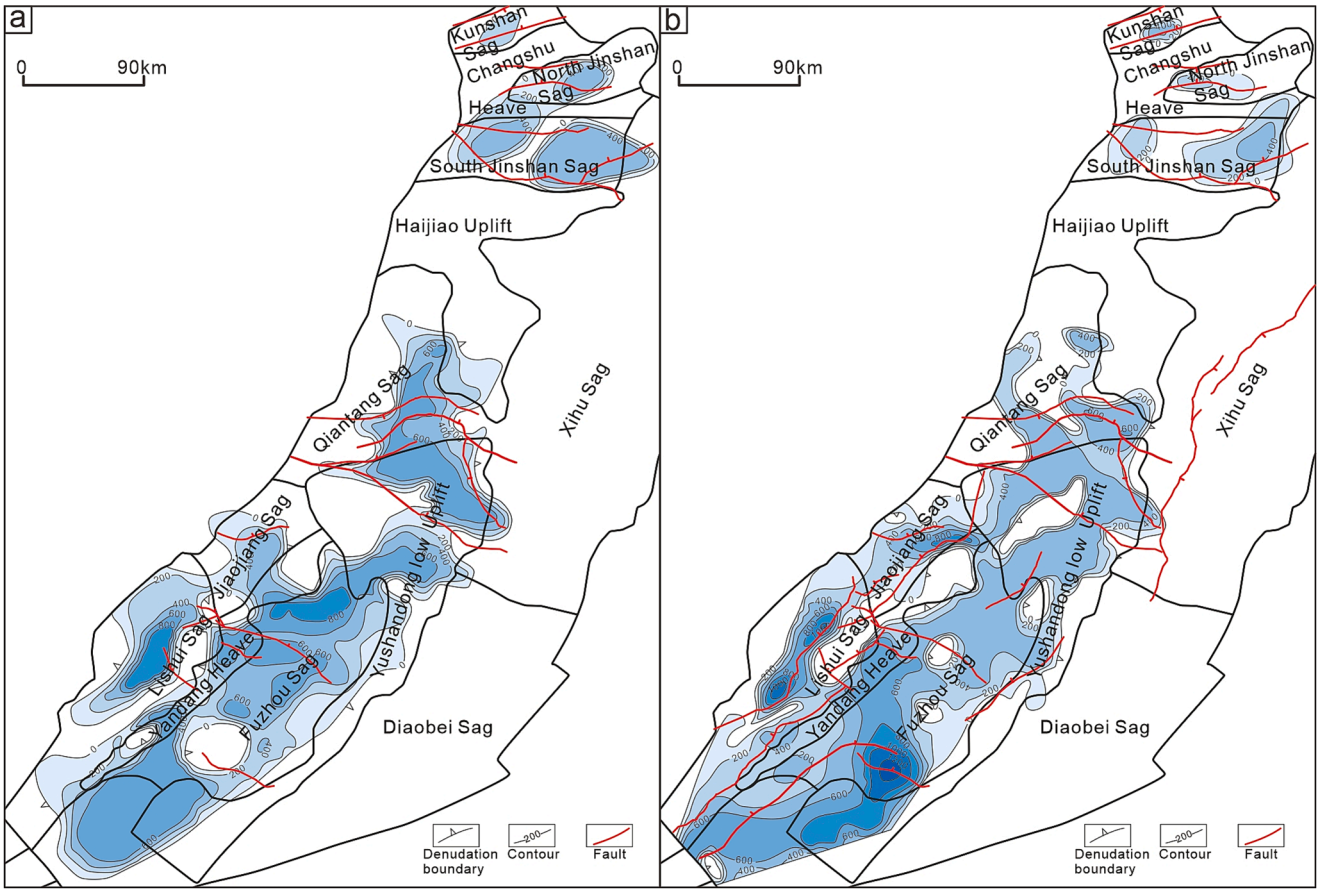

Fig. 14. (a) Thickness of the Lower-Middle Jurassic in the East China sea shelf basin. (b) The thickness of the Upper Jurassic-Lower Cretaceous in the East China sea shelf basin (Modified after Zhong et al., 2019). NWW-trending faults control the distribution of the Jurassic, while the Cretaceous mainly have an NE-trending distribution and was controlled by NE-trending faults.

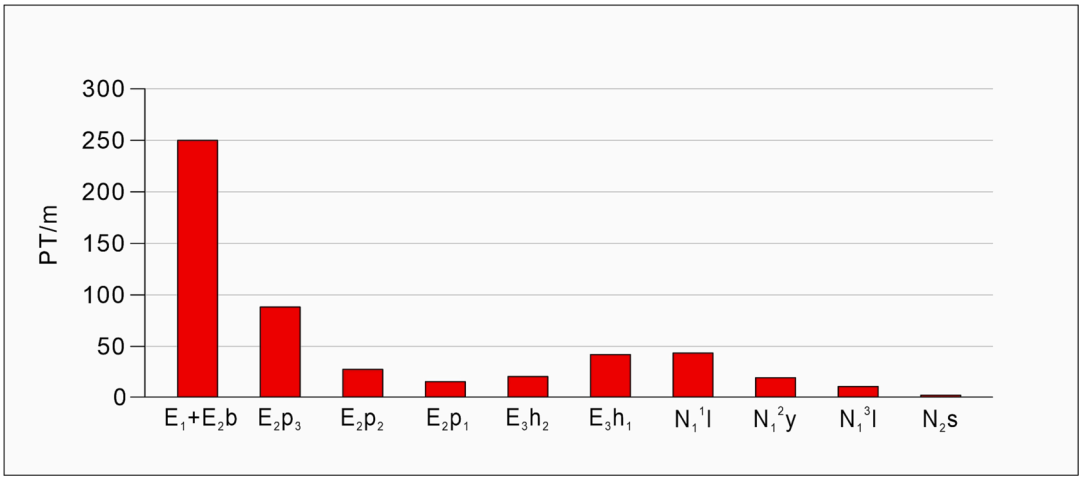

Fig. 15. Statistics of the paleo throw (PT) of the Tiantaixi fault. The Tiantaixi fault was active throughout the Cenozoic, primarily during the Paleocene and Early Eocene (E_1 + E_2b) and the lower Pinghu Formation sedimentary period (E_2p_3).

(Fig. 19c).

Quiet period (Late Oligocene–Present): the activity of the shallow fault is considerably weakened (Fig. 16), as is the strike–slip activity of the basement fault (Fig. 19d), gradually evolved into the present structure.

4.3. Inspiration of the Tiantai slope belt on the tectonic domain transformation of the ECSSB

East Asia is a triangular zone sandwiched between the western Pacific, the Paleo-Asian Ocean, and the Tethys Ocean tectonic domains. It serves as the core zone for the system transformation and tectonic superimposition of the three tectonic domains. The ECSSB, located at the

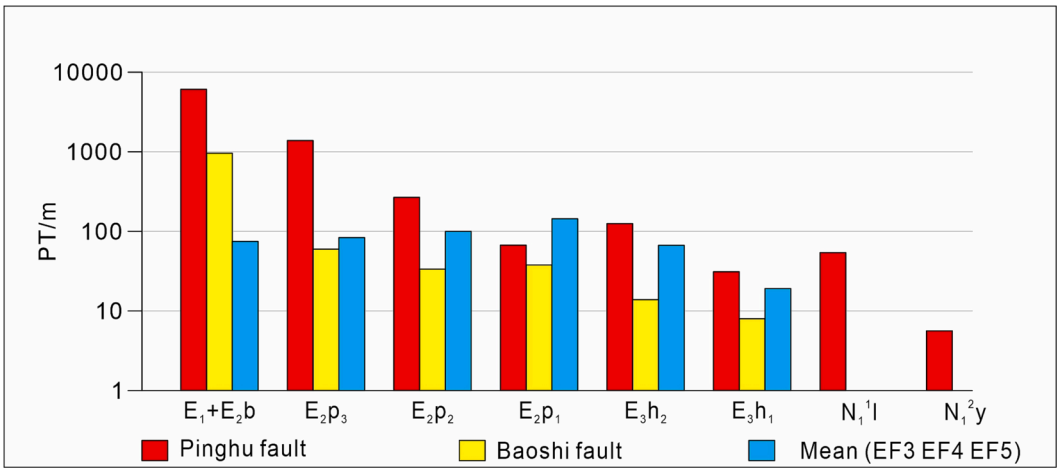

Fig. 16. Statistics of paleo throw (PT) of Pinghu and Baoshi faults. The activity of the Baoshi fault is much weaker than that of the Pinghu fault. The paleo throw of the Pinghu fault in $E_1 + E_2b$ can reach 6000 m, while the highest of the Baoshi fault is less than 1800 m. The Cenozoic activity of shallow arc fault (EF3-5) can be divided into three stages, with the relatively low activity in early Eocene ($E_1 + E_2b$), gradually enhanced in late Eocene (E_2p), and gradually weakened and stopped in Oligocene (E_3h).

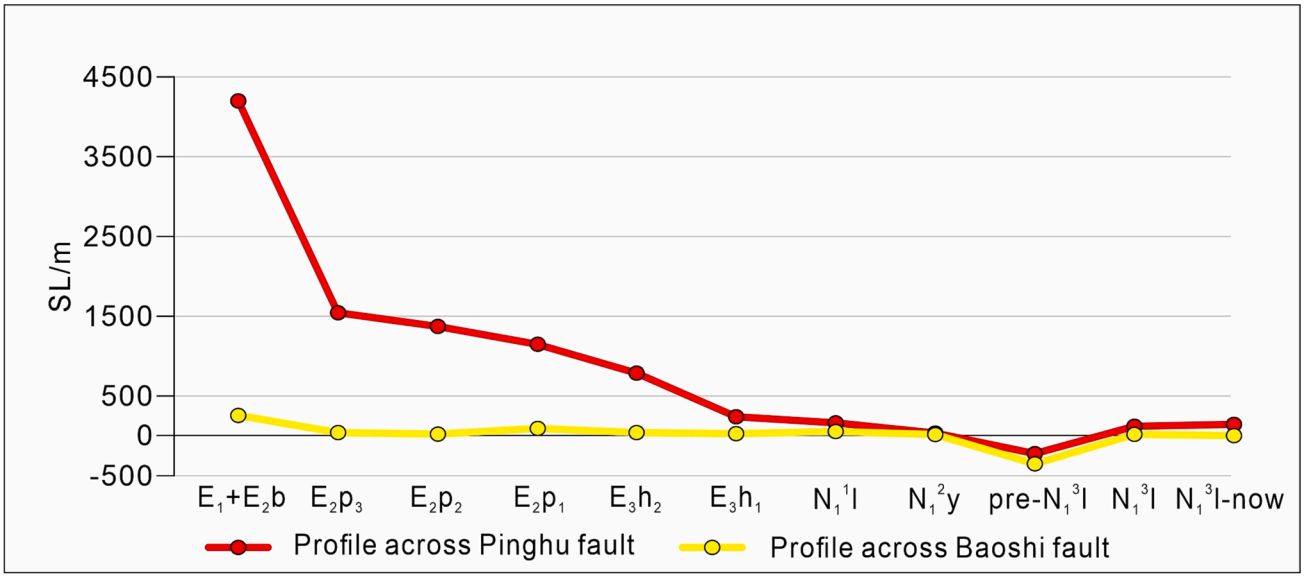

Fig. 17. Comparison of stretching length (SL) of the northern and southern part of the Tiantai slope belt. The stretching length is derived from the evolutionary profile (EE') across the Pinghu fault and the evolutionary profile (GG') across the Baoshi fault, profile positions shown in Fig. 4. The comparison results show that the extension intensity in the north of the slope is greater than that in the south, and the maximum difference of extension amount is about 3.9 km in $E_1 + E_2b$.

southeast edge of the Eurasian plate, is a component of the Western Pacific tectonic domain created by the successive Indo–Pacific dynamical systems and a part of the Tethys Ocean and ancient Asian Ocean tectonic domains (Faccenna et al., 1999; Li et al., 2012a; Liang and Wang, 2019). Consequently, the closure of the ancient Asian Ocean and the Tethys Ocean, the ongoing extension of the Indian Ocean Ridge, and the subduction of the Pacific plate are all directly linked to the formation and evolution of the ECSSB since the Mesozoic and Cenozoic periods.

The development of the tectonic system of the East Asian continent during the Mesozoic era is evident in the tectonic evolution of the Tiantai slope belt. The Qinling orogenic belt was created toward the end of the Triassic Period owing to the collision and fusion of the South China block with the North China block (Guo et al., 2017). According to regional tectonic studies, the Qinling orogenic belt entered the post-collision extension stage in the early and middle Jurassic, leading to the detachment fault zones and metamorphic core complexes of the orogenic belt under the post-extension system characterized by ultrahigh-pressure and high-pressure metamorphism (Ma et al., 2003). Combining tectonic analysis with metamorphic PTt tracks and isotopic chronology evidence shows that the extensional detachment fault formed between 200 and 170 million years ago (Suo et al., 2001). The Hangzhou Bay area also exhibits an NWW-trending normal fault that extends eastward from the Qinling orogenic belt, governing the formation of Jurassic strata (Yao, 2008). While the ancient Pacific plate subducted at a low angle and over a limited area in the early Jurassic with little impact on the East China Sea (Liu et al., 2020), the Qinling orogenic belt entered the post-collision extension stage with NE–SW extension, which can extend to the eastern sea area. An NWW-trending detachment fault system developed south of the ECSSB, controlling Jurassic sedimentation, with the Tiantaixi fault dominating the detachment fault system in the research area (Fig. 20a).

During the Early Cretaceous, a NE-trending fault occurred in the Tiantai slope belt and the NWW-trending fault slipped along the strike, causing the NE-trending fault strike to change and become an arc fault.

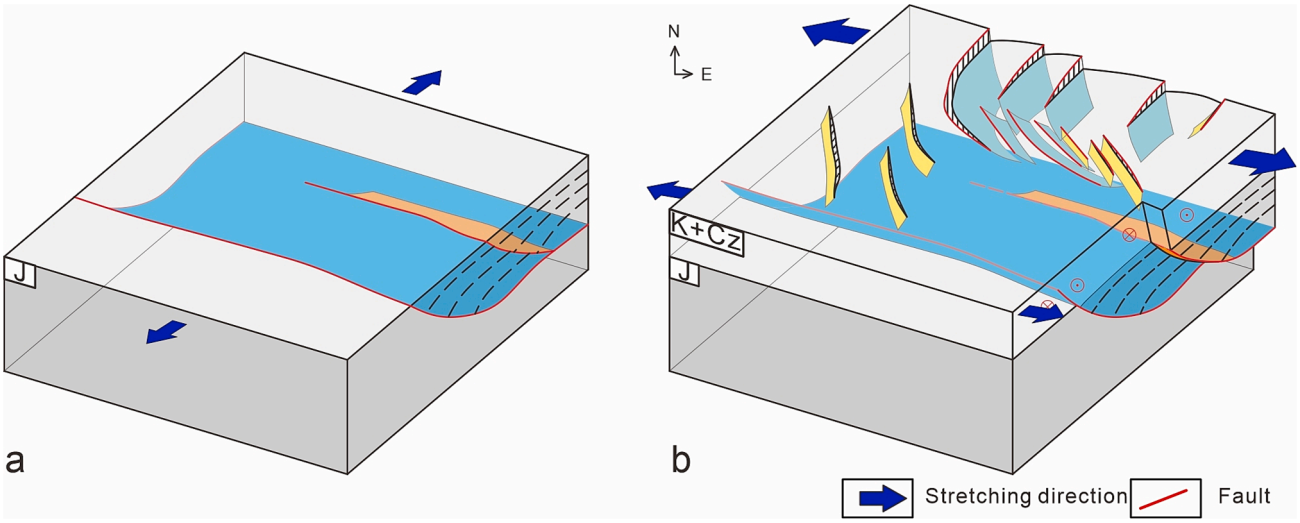

Fig. 18. (a) Detachment fault systems and (b) Accommodation fault systems of the Tiantai slope belt. The difference in the size of the blue arrows represents the difference of the strength of the strain.

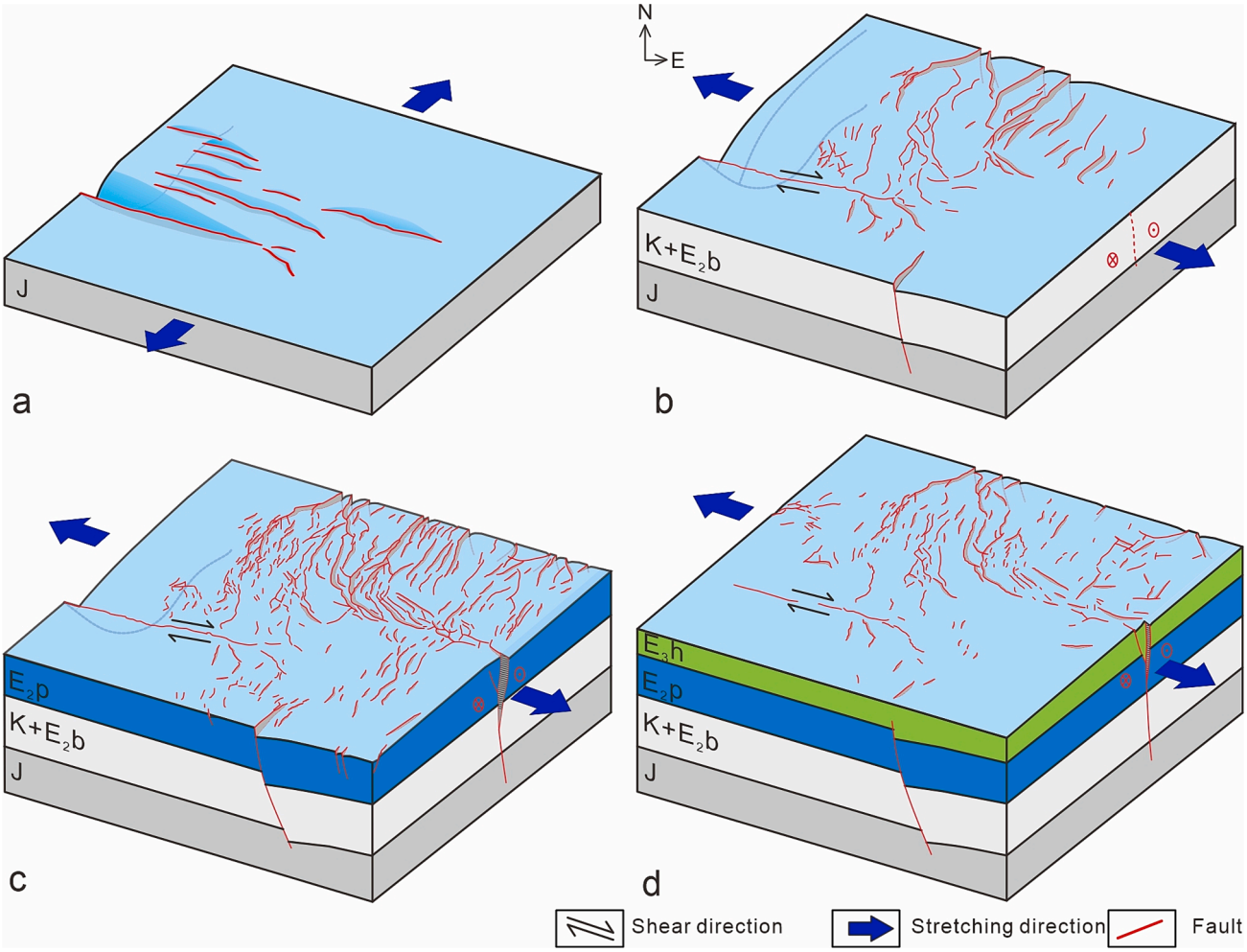

Fig. 19. Schematic diagram of the development and evolution of the Tiantai slope belt. (a) Incubation period (Jurassic), (b) Initial stage (Cretaceous–Early Eocene Epoch), (c) Maturity period (Late Eocene), (d) Quiet period (Late Oligocene–Present).

This change in fault strike indicates a shift in the stress direction of the Tiantai slope belt during the Early Cretaceous. The slab rollback of the Western Pacific plate began around 145 Ma (Wu et al., 2019; Ma and Xu, 2021), during the Early Cretaceous (130–120 Ma), the Western Pacific plate transformed into high-angle subduction and rollback with the maximum rollbacking rate (Zhu and Xu, 2019; Liu et al., 2019; Fang

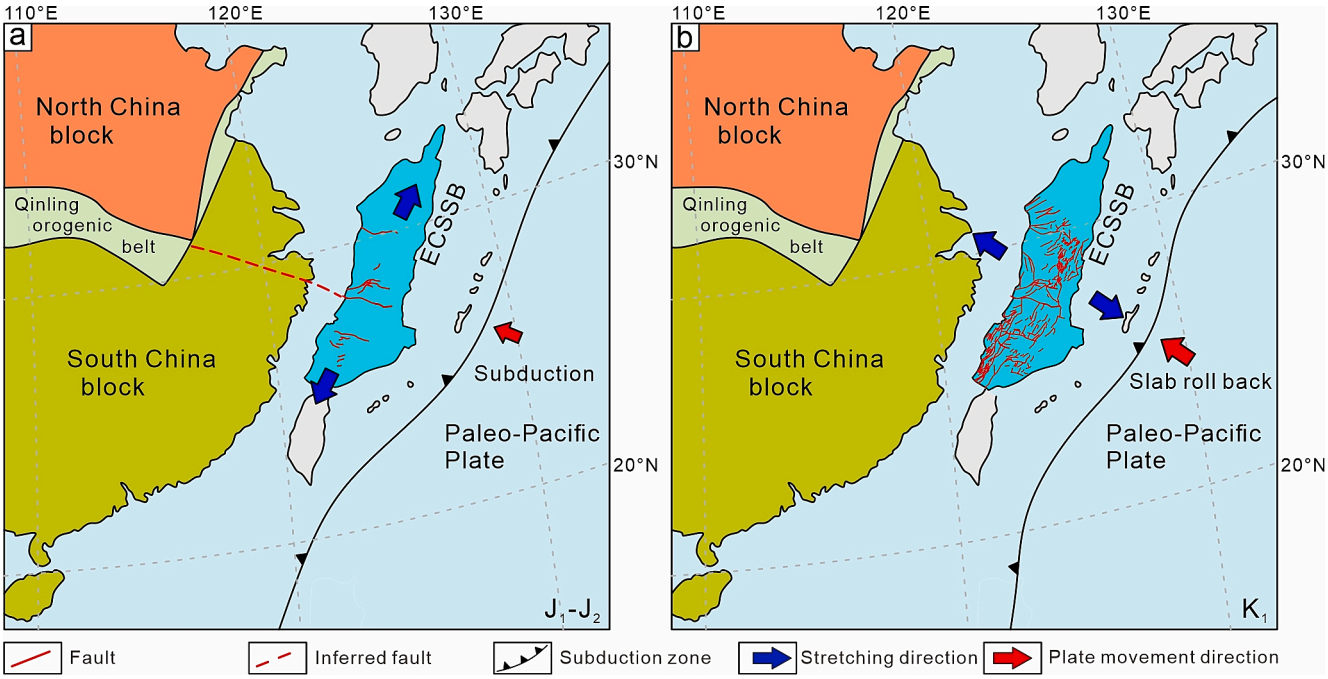

Fig. 20. The transformation of the stress field in the Early–Middle Jurassic (a) and Cretaceous (b) of the ECSSB. a. The ancient Pacific plate subducted at a low angle with little impact on the East China Sea in the early and middle Jurassic, while the Qinling orogenic belt entered the post-collision extension stage with NE-SW extension, which can extend to the eastern sea area. b. In the early Cretaceous, the Western Pacific plate transformed into a high-angle subduction and rollback, placing the ECSSB in a back-arc extensional environment, forming a NE-trending structural feature.

et al., 2021), which placed the North China Craton in the extensional background and led to the craton's destruction. Large-scale magmatism, mantle arching, lithosphere thinning, and extension occurred due to the subduction and rollback of the western Pacific plate, placing the East Asian continental margin in a back-arc extensional environment. This led to the formation of numerous rift basins, creating an important trench arc basin system near the western Pacific Ocean, an NNE-trending structural system in East Asia, and a seismic–volcanic activity belt (Bao et al., 2013; Faccenna et al., 1999; Li et al., 2012a; Ma et al., 2022; Mueller et al., 2016; Suo et al., 2014; Isozaki et al., 2010). In this context, the ECSSB entered the back-arc rift evolution stage of the Pacific tectonic system, building upon the Jurassic continental marginal depression. The early continental marginal depression basin underwent superposition and reconstruction, forming an NE–NNE-trending structural feature (Fig. 20b).

5. Conclusion

(1) The Tiantai slope belt primarily exhibits two groups of faults in the NE and NWW directions. The NE- trending faults primarily comprise shovel-type normal faults that originated during the Early Cretaceous. The NWW-trending basement faults were identified, represented by the Tiantaixi detachment fault system, which have been active since the Jurassic.

(2) The fault system in the Tiantai slope belt is complex, with multiple-stage faults superimposing to form an intricate structural system. The NWW-trending faults during the Jurassic were detachment fault systems. The stress direction shifted during the Early Cretaceous, with greater extension strength observed in the north of the Tiantai slope belt compared to the south. The difference in extension strength between the south and the north led to the strike–slip activity of NWW-trending basement faults to accommodate the deformation, resulting in the formation of shallow arc faults in the hanging wall. The tectonic evolution of the Tiantai slope belt can be divided into four stages: the incubation period (Jurassic), the initial period (Cretaceous-Earlyocene Epoch), the mature period (Late Eocene), and the quiet period (Late Oligocene-Present).

(3) The ECCSB underwent a system shift from the EW-trending Tethys tectonic domain to the NE-trending western Pacific tectonic domain throughout the Mesozoic. The tectonic evolution of the Tiantai slope belt indicates that the East China Sea Shelf Basin completed the transition from the Paleo-Tethys tectonic domain to the Pacific tectonic domain in the Early Cretaceous. Following the Jurassic continental marginal depression, the ECCSB entered the back-arc rift evolution stage of the Pacific tectonic system.

CRediT authorship contribution statement

Xinxin Liang: Conceptualization, Methodology, Writing – original draft, Writing – review & editing. **Shi Chen:** Supervision, Funding acquisition, Writing – review & editing. **Bingshan Ma:** Writing – review & editing. **Baotong Ding:** Software. **Yuanyuan Liang:** Validation. **Xingguo Song:** Validation. **Jianxun Zhou:** Formal analysis. **Yixin Yu:** Resources. **Lang Yu:** Investigation.

Declaration of Competing Interest

The authors declare that they have no known competing financial interests or personal relationships that could have appeared to influence the work reported in this paper.

Data availability

Data will be made available on request.

Acknowledgments

This study was financially supported by the National Natural Sciences Foundation of China (Grant No. 42272157).

References

Bao, H.Y., Guo, Z.F., Zhang, L.L., Huang, Y.P., 2013. Tectonic Dynamics of Eastern China Since the Formation of the Pacific Plate. Adv. Earth Sci. 28, 337–338 in Chinese with English abstract.

Chen, S.Z., 2003. Main geological characteristics and gas exploration directions in East China Sea Basin. China Offshore Oil and Gas (Geology). 17, 8–15 in Chinese with English abstract.

Cui, X., Dai, L.M., Li, S.Z., Guo, L.L., Suo, Y.H., 2019. Control of strike-slip and pull-apart processes to tectonic transition of the southern East China Sea Shelf Basin. Geol. J. 54, 850–861.

Cukur, D., Horozal, S., Kim, D.C., Han, H.C., 2011. Seismic stratigraphy and structural analysis of the northern East China Sea Shelf Basin interpreted from multi-channel seismic reflection data and cross-section restoration. Mar. Pet. Geol. 28, 1003–1022.

Cukur, D., Horozal, S., Lee, G.H., Kim, D.C., Han, H.C., 2012. Timing of trap formation and petroleum generation in the northern East China Sea Shelf Basin. Mar. Pet. Geol. 36, 154–163.

Dai, L.M., Li, S.Z., Lou, D., Liu, X., Suo, Y.H., Yu, S., 2014. Numerical modeling of Late Miocene tectonic inversion in the Xihu Sag, East China Sea Shelf Basin, China. J. Asian Earth Sci. 86, 25–37.

Faccenna, C., Giardini, D., Davy, P., Argentieri, A., 1999. Initiation of subduction at Atlantic-type margins: Insights from laboratory experiments. J. Geophys. Res. Solid Earth 104, 2749–2766.

Fang, W., Dai, L.Q., Zheng, Y.F., Zhao, Z.F., Ma, L.T., Zhao, K., 2021. Identification of Jurassic mafic arc magmatism in the eastern North China Craton: Geochemical evidence for westward subduction of the Paleo-Pacific slab. GSA Bull. 133, 1404–1420.

Feng, X.J., Cai, D.S., Wang, C.X., Gao, L., 2003. The Meso-Cenozoic tectonic evolution in East China Sea Shelf Basin. China Offshore Oil and Gas 17, 35–39 in Chinese with English abstract.

Guo, R.H., Li, S.Z., Suo, Y.H., Wang, Q., Zhao, S.J., Wang, Y.N., Liu, X.G., Zhou, Z.Z., Li, J., Lan, H.Y., Wang, P.C., Guo, L.L., 2017. Indentation of North China Block into Greater South China Block and Indosinian Orocline. Earth Sci. Front. 24, 171–184 in Chinese with English abstract.

Hou, F.H., Zhang, X.H., Li, G., Li, S.Z., Wen, Z.H., Li, R.H., 2015. From passive continental margin to active continental magin: basin recordings of Mesozoic tectonic regime transition of the East China Sea Shelf Basin. Oil Geophys. Prospecting. 50, 980–990 in Chinese with English abstract.

Isozaki, Y., Aoki, K., Nakama, T.,Yanai, S., 2010. New insight into a subduction-related orogen: A reappraisal of the geotectonic framework and evolution of the Japanese Islands. Gondwana Research.

Jiao, R.C., Yin, W.R., 1987. Discussion on the controlling effect of the Zhoushan- Guotou fault zone in the East China Sea and its extension to the continental area. Shanghai Land & Resources 25–41 in Chinese with English abstract.

Li, S.Q., 2000. Cenozoic basin geological tectonic feature and evolution in Xihu Trough, East China Sea. Offshore Oil 104, 8–14 in Chinese with English abstract.

Li, Z.G., Gong, J.M., Cao, Y.C., Wang, J., Wang, W.C., Li, G., 2015. Comparison of sedimentary characteristics of the Mesozoic in Southern East China Sea and adjacent uplifting areas. Mar. Geol. Quat. Geol. 35, 29–35 in Chinese with English abstract.

Li, Z.X., Li, X.H., Chung, S.L., Lo, C.H., Xu, X., Li, W.X., 2012b. Magmatic switch-on and switch-off along the South China continental margin since the Permian: Transition from an Andean-type to a Western Pacific-type plate boundary. Tectonophysics 532–535, 271–290.

Li, S.Z., Santosh, M., Zhao, G.C., Zhang, G.W., Jin, C., 2012a. Intracontinental deformation in a frontier of super-convergence: A perspective on the tectonic milieu of the South China Block. J. Asian Earth Sci. 49, 313–329.

Liang, R.B., 2012. The distribution of Mesozoic in the Southern part of the East China Sea Shelf Basin. Offshore Oil. 32, 18–22 in Chinese with English abstract.

Liang, J., Wang, H., 2019. Cenozoic tectonic evolution of the East China Sea Shelf Basin and its coupling relationships with the Pacific Plate subduction - ScienceDirect. J. Asian Earth Sci. 171, 376–387.

Liu, J.G., Cai, R.H., Pearson, D.G., Scott, J.M., 2019. Thinning and destruction of the lithospheric mantle root beneath the North China Craton: A review. Earth Sci. Rev. 196, 102873.

Liu, J.S., Xu, H.Z., Jiang, Y.M., Wang, J., He, X.J., 2020. Mesozoic and Cenozoic basin structure and tectonic evolution in the East China Sea basin. Acta Geol. Sin. 94, 675–691 in Chinese with English abstract.

Ma, B.S., Qi, J.F., Wu, G.H., Ren, J.Y., Yang, L.L., Sun, T., Chen, S., Chen, W.C., Ge, J.W., 2022. Structural Variability and Rifting Process of the Segmented Cenozoic Pearl River Mouth Basin. Northern Continental Margin of the South China Sea 96, 2074–2092.

Ma, Q., Xu, Y.G., 2021. Magmatic perspective on subduction of Paleo-Pacific plate and initiation of big mantle wedge in East Asia. EarthScience Rev. 213, 103473.

Ma, C.Q., Yang, K.G., Ming, H.L., Lin, G.C., 2003. The timing of tectonic transition from compression to extension in Dabieshan: Evidence from Mesozoic granites. Sci. China, Ser. D 47, 817–827 in Chinese with English abstract.

Mueller, R.D., Seton, M., Zahirovic, S., Williams, S.E., Matthews, K.J., Wright, N.M., Shephard, G.E., Maloney, K.T., Barnett-Moore, N., Hosseinpour, M., Bower, D.J., Cannon, J., 2016. Ocean basin evolution and global-scale plate reorganization events since Pangea breakup. Annu. Rev. Earth Planet. Sci. 44, 107–138.

Suo, Y.H., Li, S.Z., Yu, S., Somerville, I.D., Liu, X., Zhao, S.J., Dai, L.M., 2014. Cenozoic tectonic jumping and implications for hydrocarbon accumulation in basins in the East Asia Continental Margin. J. Asian Earth Sci. 88, 28–40.

Suo, S.T., Zhong, Z.Q., You, Z.D., 2001. Extensional tectonic framework of the Dabie-Sulu UHP-HP metamorphic belt, Central China, and Its geodynamical significance. Acta Geol. Sin. 75, 14–24 in Chinese with English abstract.

Tang, X.J., Jiang, Y.M., Zhang, J.P., Wang, C., He, X.J., Yang, M., 2019. Fault characteristic and its control on traps of fault structural layer in the Northern Pinghu Slope Belt, Xihu Sag, East China Sea Shelf Basin. Mar. Geol. Front. 35, 34–43 in Chinese with English abstract.

Wang, F.W., Chen, D.X., Du, W.L., Zeng, J.H., Wang, Q.C., Tian, Z.Y., Chang, S.Y., Jiang, M.Y., 2021. Improved method for quantitative evaluation of fault vertical sealing: A case study from the eastern Pinghu Slope Belt of the Xihu Depression, East China Sea Shelf Basin. Mar. Pet. Geol. 132, 1–22.

Wang, C., Tang, X.J., Jiang, Y.M., He, X.J., Tan, S.Z., 2020. Characteristics of the structural transfer zone of northern Tiantai slope in Xihu Sag of the East China Sea Basin and their petroleum geological significances. Mar. Geol. Quat. Geol. 40, 93–105 in Chinese with English abstract.

Wu, F.Y., Yang, J.H., Xu, Y.G., Wilde, S.A., Walker, R.J., 2019. Destruction of the North China craton in the Mesozoic. Annu. Rev. Earth Planet. Sci. 47, 173–195.

Xu, F., 2012. Characteristics of caenozoic structure and tectonic migration of the East China Shelf Basin. J. Oil Gas Technol. 34, 1–7 in Chinese with English abstract.

Xu, Q.J., Liu, S.F., Wang, Z.F., Zhang, B., 2019. Provenance of the East Guangdong Basin and Yong'an Basin in southeast China: Response to the Mesozoic tectonic regime transformation. J. Asian Earth Sci. 185, 1–17.

Yang, C.Q., Yang, C.S., Sun, J., Ynag, Y.Q., 2019a. Mesozoic evolution and dynamics transition in Southern Shelf Basin of the East China Sea. J. Jilin Univ. 49, 139–153 in Chinese with English abstract.

Yang, Y.Q., Yang, C.Q., Yang, C.S., Sun, J., 2019b. Mesozoic fault system in the Southern East China Sea Shelf Basin and its bearing on basin structures. Mar. Geol. Quat. Geol. 39, 52–61 in Chinese with English abstract.

Yang, C.S., Yang, C.Q., Yang, Y.Q., Sun, J., Yan, Z.H., Wang, J.Q., 2020. Meo-Cenozoic deformation and dynamic mechanism of the ocean-continent transitional zone in the East China Sea. Mar. Geol. Quat. Geol. 40, 71–84 in Chinese with English abstract.

Yao, Q., 2008. Neotectonics of NW-SE trending faults in Hangzhou Bay. Zhejiang University, Zhejiang, China in Chinese with English abstract.

Yu, X.Q., Wu, G.G., Zhang, D., Di, Y.J., Zang, W.S., Zhang, X.X., Wang, Q.F., 2005. Research progress of Mesozoic tectonic system transformation in Southeast China. Prog. Nat. Sci. 15, 17–24 in Chinese with English abstract.

Zhang, G.H., Li, S.Z., Suo, Y.H., Zhang, J.P., 2016a. Cenozoic positive inversion tectonics and its migration in the East China Sea Shelf Basin. Geol. J. 51, 176–187.

Zhang, J.P., Zhang, T., Tang, X.J., 2014a. Basin type and dynamic environment in the East China Sea Shelf Basi. Acta Geol. Sin. 88, 2033–2043 in Chinese with English abstract.

Zhang, J.P., Li, S.Z., Suo, Y.H., 2016b. Formation, tectonic evolution and dynamics of the East China Sea Shelf Basin. Geol. J. 51, 162–175.

Zhang, Y.Q., Xu, X.B., Jia, D., Shu, L.S., 2009. Deformation record of the change from Indosinian collision-related tectonic system to Yanshanian subduction-related tectonic system in South China during the Early Mesozoic. Earth Sci. Front. 16, 234–247 in Chinese with English abstract.

Zhang, S.L., Zhang, J.P., Tang, X.J., Zhang, T., 2014b. Geometry characteristic of the fault system in Xihu Sag in East China Sea and its formation mechanism. Mar. Geol. Quat. Geol. 34, 87–94 in Chinese with English abstract.

Zhong, K., Wang, X.F., Zhang, T., Zhang, M.Q., Fu, X.W., Guo, M., 2019. Distribution of residual Mesozoic basins and their exploration potential in the western depression zone of East China Sea Shelf Basin. Mar. Geol. Quat. Geol. 39, 41–51 in Chinese with English abstract.

Zhu, R.X., Xu, Y.G., 2019. The subduction of the west Pacific plate and the destruction of the North China Craton. Sci. China Earth Sci. 62, 1340–1350 in Chinese with English abstract.